



HAL
open science

Local Optimization Algorithms for Maximum Planar Subgraph

Gruia Călinescu, Sumedha Uniyal

► **To cite this version:**

Gruia Călinescu, Sumedha Uniyal. Local Optimization Algorithms for Maximum Planar Subgraph. 2024. hal-04629835v2

HAL Id: hal-04629835

<https://hal.science/hal-04629835v2>

Preprint submitted on 13 Aug 2024

HAL is a multi-disciplinary open access archive for the deposit and dissemination of scientific research documents, whether they are published or not. The documents may come from teaching and research institutions in France or abroad, or from public or private research centers.

L'archive ouverte pluridisciplinaire **HAL**, est destinée au dépôt et à la diffusion de documents scientifiques de niveau recherche, publiés ou non, émanant des établissements d'enseignement et de recherche français ou étrangers, des laboratoires publics ou privés.

1 Local Optimization Algorithms for Maximum 2 Planar Subgraph

3 **Gruia Călinescu @ ORCID**

4 Department of Computer Science, Illinois Institute of Technology, USA.

5 **Sumedha Uniyal @ ORCID**

6 Department of Computer Science, Aalto University, Finland

7 — Abstract —

8 Consider the NP-hard problem of, given a simple graph G , to find a planar subgraph of G with the
9 maximum number of edges. This is called the Maximum Planar Subgraph problem and the best
10 known approximation is $4/9$ and is obtained by sophisticated Graphic Matroid Parity algorithms.
11 Here we show that applying a local optimization phase to the output of this known algorithm
12 improves this approximation ratio by a small $\epsilon = 1/747 > 0$. This is the first improvement in
13 approximation ratio in more than a quarter century. The analysis relies on a more refined extremal
14 bound on the Lovász cactus number in planar graphs, compared to the earlier (tight) bound of [5, 8].

15 A second local optimization algorithm achieves a tight ratio of $5/12$ for Maximum Planar Subgraph
16 without using Graphic Matroid Parity. We also show that applying a greedy algorithm before this
17 second optimization algorithm improves its ratio to at least $91/216 < 4/9$. The motivation for not
18 using Graphic Matroid Parity is that it requires sophisticated algorithms that are not considered
19 practical by previous work. Also, we could not find any implementation ¹. The best previously
20 published [7] approximation ratio without Graphic Matroid Parity is $13/33 < 5/12$.

21 **2012 ACM Subject Classification** Theory of computation → Approximation algorithms analysis

22 **Keywords and phrases** planar graph, maximum subgraph, approximation algorithm, matroid parity,
23 local optimization

24 **Digital Object Identifier** 10.4230/LIPIcs.ESA.2024.3

25 **Funding** Gruia Călinescu’s work performed in part while visiting Northwestern University. Sumedha’s
26 work performed in part at Aalto University, Finland, and in part at Northwestern University, United
27 States of America. She was supported by the Academy of Finland (grant agreement number 314284).
28 *Sumedha Uniyal*: Sumedha Uniyal passed away in February 2020. Her husband, Prajna Uniyal,
29 email uniyal.prajna@gmail.com, has approved this submission.

30 **Acknowledgements** Gruia thanks Michael Pelsmajer for many comments that improved the presen-
31 tation. Gruia thanks the anonymous SODA 2024 reviewer B who suggested using a positive linear
32 combination (instead of case analysis) when computing the ϵ -improvement of Algorithm MTLK4,
33 which lead to a slightly simpler proof with a bigger ϵ . Gruia also thanks Konstantin Makarychev for
34 hints on finding the best linear combination.

¹ After this paper was accepted by ESA 2024, We found out from Matthias Stallmann about
<https://github.com/Arkhist/Graphic-Matroid-Parity>



1 Introduction

Maximum Planar Subgraph (MPS) is the following problem: given a graph G , find a planar subgraph of G with the maximum number of edges. MPS is known to be NP-complete [24] and APX-hard [5], meaning that there exists a small $\epsilon > 0$ such that a polynomial-time algorithm with approximation ratio of at least $1 - \epsilon$ for MPS implies that $P = NP$. In this paper all graphs are undirected, nonempty, finite, simple graphs unless otherwise noted.

Besides theoretical appeal, MPS has applications in circuit layout, facility layout, and graph drawing (see [17, 31, 27, 23, 14, 12, 21] and the references contained there). Poranen [27] uses simulated annealing and interestingly reports that using the output of better approximation algorithms as the start of simulated annealing obtains better practical results. Chimani, Klein, and Wiedera [13] also report benefits of using better approximation algorithms for MPS.

We assume that the reader has basic knowledge of planar graphs and approximation algorithms. For a quarter century, the best known approximation algorithm for MPS has a tight approximation ratio² of $4/9$ [5] and uses polynomial-time algorithms for Graphic Matroid Parity³ to construct a maximum triangular cactus (a graph all of whose blocks⁴ are triangles⁵), followed by adding edges to connect the components of this cactus without creating any new cycles. Graphic Matroid Parity has polynomial-time algorithms [26, 25, 9, 18, 19] and allows us to find a triangular cactus with maximum number of triangles.

In this paper we show that applying a local optimization phase after finding a maximum triangular cactus achieves an approximation ratio of $(4/9) + \epsilon$, for a small $\epsilon > 0$. A second local optimization algorithm achieves a tight ratio of $5/12$ for MPS without using Graphic Matroid Parity. We also show that applying a “greedy” algorithm before this second local optimization algorithm improves its ratio to at least $91/216$. This variant has an upper limit of $3/7 < 4/9$ on its approximation ratio. The motivation for not using Graphic Matroid Parity is that it requires sophisticated algorithms that are not considered practical by Chimani and Wiedera [14]⁶. The best previously published [7] approximation ratio without Graphic Matroid Parity is $13/33 < 5/12$.

Besides these theoretical guarantees, both of our local optimizations “make sense” (since each local improvement step increases the size of the output by one) and can be used in heuristics, or as a starting point of simulated annealing. Other ideas that make sense are further discussed in Conclusions (Section 6).

1.1 Previous Theoretical Work

A planar graph on n vertices has at most $3n - 6$ edges. As we can assume that the input graph is connected (or else we can run an algorithm separately on the connected components of the input), simply outputting a spanning tree achieves a tight approximation ratio of $1/3$. Dyer, Foulds, and Frieze [16] proved that the Maximal Planar Subgraph, which simply outputs an inclusion-maximal planar subgraph, has performance ratio $1/3$. Cimikowski [15] proved that the heuristics of Chiba, Nishioka, and Shirakawa [10] and of Cai, Han, and

² *tight* in this paper means that there are matching examples for the approximation ratio of the algorithm

³ See Section 2 for the exact definition

⁴ We use the standard definition of *block*, explicitly stated in Section 2

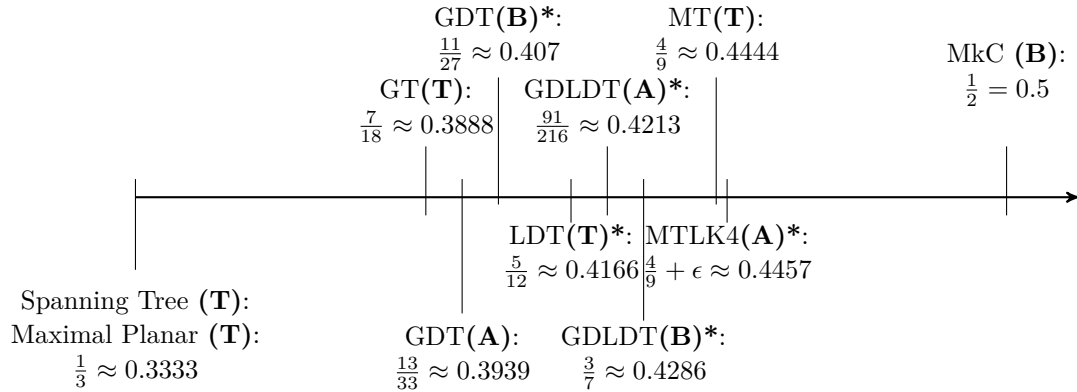
⁵ A simple graph is a *cactus* if any two distinct simple cycles have at most one vertex in common. A triangular cactus as defined by us is a cactus.

⁶ Also, we could not find any implementation.

74 Tarjan [2] have performance ratios not exceeding $1/3$.

75 Călinescu, Fernandes, Finkler, and Karloff [5] were the first to improve this. Their first
 76 algorithm (GT, from Greedy-Triangles) (greedily) adds triangles, as long as the graph stays a
 77 triangular cactus. Then the algorithm greedily adds edges connecting the components of the
 78 cactus, without creating any new cycles. This “connecting” phase appears at the end of all
 79 the approximation algorithms and we will not mention it from now on. The GT algorithm has
 80 a tight approximation ratio of $7/18$. Their second algorithm (MT, from Maximum-Triangular
 81 Cactus) employs exact algorithms for Graphic Matroid Parity (i.e., [25]) to construct a
 82 triangular cactus with a maximum number of triangles. This algorithm achieves a tight
 83 approximation of $4/9$, and the analysis is long and complicated. Another claim of the $4/9$
 84 ratio was sent in a personal communication in 1996 or 1997 by Danny Raz, and is also proven
 85 in Chalermsook, Schmid, and Uniyal [8]⁷; these proofs are also long and/or complicated.

86 Poranen [28] proposes two new approximation algorithms but their ratio is below $4/9$ [11].
 87 Chalermsook and Schmid [7] obtain a $13/33$ ratio without using Graphic Matroid Parity.
 88 Note that $13/33 > 7/18$. We have examples showing that this algorithm has ratio at most
 89 $11/27 < 5/12$. See Figure 1 for a graphical representation of approximation ratios.

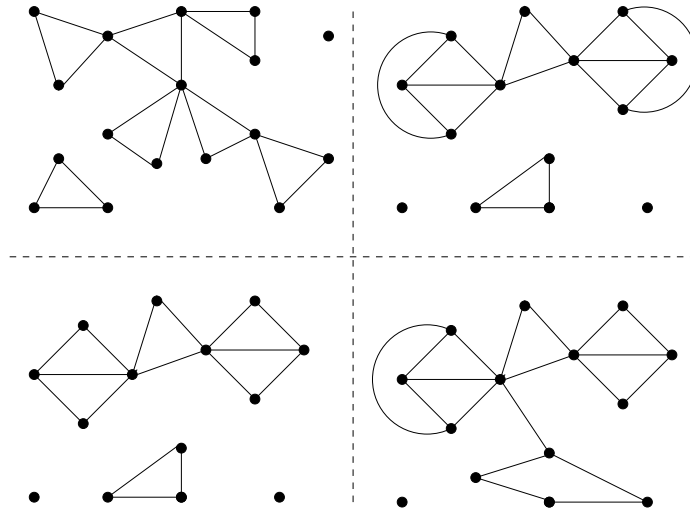


■ **Figure 1** Ratios for various approaches. **(T)** says that the result is tight with matching example. **(A)** says that an algorithm is proven to achieve that ratio. **(B)** states an upper bound for the approximation ratio of an algorithm. New results marked by *.

90 **1.2 Techniques discussion**

91 A graph A is a kt -structure if every block in every non-trivial connected component of A
 92 is either a K_4 or a triangle. A diamond is the graph resulting from deleting any single
 93 edge from a K_4 . A graph A is a dt -structure if every block in every non-trivial connected
 94 component of A is either a diamond or a triangle. A graph A is a 4 -structure if every block
 95 in A has at most 4 vertices. All 4 -structures are planar graphs. See Figure 2 for illustrations.

⁷ [8] also has the sentence “Therefore, combining this with our bound implies that local search arguments are sufficient to get us to a $\frac{4}{9} + \epsilon$ approximation for MPS”, but no proof for this sentence; their previous arguments give a $\frac{4}{9} - \epsilon$ approximation.



■ **Figure 2** In the upper left, a triangular cactus. In the upper right, a kt-structure. In the lower left, a dt-structure. In the lower right, a 4-structure.

96 4-Structures can have more edges than triangular cacti, but finding a 4-structure with
 97 maximum number of edges is known to be NP-hard [4] (easy reduction from 3D-Matching [20]).
 98 It is known [3] that even if we fix k and allow blocks of size up to k in our output, and could
 99 find the k -structure with maximum number of edges and planar blocks (algorithm MkC), we
 100 would still get an approximation ratio of smaller than $1/2$.

101 Local optimization is a powerful technique for unweighted maximization problems. For
 102 example, Lee, Sviridenko, and Vondrák [22] prove that a basic local optimization algorithm
 103 achieves a $(1 - \epsilon)$ -approximation for Matroid Parity, a generalization of Graphic Matroid
 104 Parity that is NP-hard [29]. Using local optimization for MPS was suggested by [8].

105 Our first algorithm, denoted by MTLK4 (Maximum-Triangular-Local-K4) from now on,
 106 starts with a maximum triangular cactus and simply replaces, as long as we still have a
 107 kt-structure, at most two triangles by a K_4 . Previous approximation algorithms for MPS
 108 have not been able to exploit K_4 's in getting a better approximation ratio, and in fact our
 109 analysis giving that the approximation ratio of MTLK4 is at least $(4/9) + \epsilon$ is complicated
 110 and not tight⁸. The analysis relies on Theorem 5, which gives a more refined extremal bound
 111 on the Lovász cactus number in planar graphs, compared to the earlier (tight) bound of
 112 [5, 8].

113 The algorithm of Chalermsook and Schmid [7] (which we call GDT, from Greedy-
 114 Diamonds-Triangles) consists of greedily adding diamonds followed by greedily adding
 115 triangles (while staying a dt-structure), and has approximation ratio between $13/33$ and
 116 $11/27$. Our $5/12$ approximation ratio of our second local optimization algorithm, denoted by
 117 LDT (Local-Diamonds-Triangles) from now on, is based on the fact that LDT does “break”
 118 diamonds to add more diamonds, assuming a triangle is left from our broken diamond. While
 119 this $5/12$ -approximation is tight, it can be improved by greedily adding diamonds (while
 120 staying a dt-structure)⁹, followed by LDT. We call this algorithm GDLDT. We prove that
 121 GDLDT has an approximation ratio between $91/216$ and $3/7$.

122 While our algorithms are fairly simple, their analyses are long and complicated. The

⁸ We believe that another page of arguments will make our ϵ a very little bit bigger.

⁹ This is exactly the start of the GDT algorithm of [7].

123 reader may want to start with the (7/18)-approximation of [5] (also presented in [4]) for a
 124 simple non-trivial algorithm with a somewhat simple analysis.

125 One can also use local optimization to approximate Graphic Matroid Parity, as described
 126 in [22]. As pointed out in [8], this leads to a $4/9 - \epsilon$ approximation for MPS, as outlined below.
 127 The local optimization algorithm used by [22], adapted to our terminology, replaces sets of k
 128 triangles by sets of $k + 1$ triangles, as long as it keeps a triangular cactus. We have (so far
 129 unpublished, and involving a different set of authors) evidence that swapping two triangles
 130 for one gives a ratio of at least 11/27. Theorem 1.1 of [8] also mentions a 2-swap algorithm,
 131 but it swaps only triangles of a plane graph and is not analyzed as an MPS algorithm. Let
 132 n be the number of vertices in the input graph, and M be the number of triangles in the
 133 input graph. The analysis of [22] requires $k = 5^{\lceil 1/(2\epsilon) \rceil}$ to achieve a $(1 - \epsilon)$ -approximation for
 134 Matroid Parity. To achieve a 5/12 approximation for MPS, one would need an $\epsilon = 1/4$ above:
 135 if the optimum is triangulated and the maximum triangular cactus has $n/3$ triangles (which
 136 we know that it can happen, from [5]), then we need a triangular cactus with almost $n/4$
 137 triangles in the algorithm's cactus to get a ratio of 5/12, which means we must approximate
 138 Graphic Matroid Parity with a factor of 3/4. Directly using the analysis of [22] gives an
 139 $O(M^{25})$ -time algorithm. We do not fully understand [1] and maybe it provides a better
 140 analysis of the swapping heuristics and achieves a $O(n^{4+3/\epsilon})$ running time. This would be
 141 $O(n^{16})$ time to get a ratio of 5/12 for MPS. By comparison, our LDT algorithm has an
 142 implementation that runs in $O(n^5)$ time.

143 2 Preliminaries

144 Generally speaking we follow West [32] for terminology and notation. Given a graph
 145 $G = (V, E)$ and $V' \subseteq V$, we denote by $G[V']$, the *induced* subgraph of G with vertex set given
 146 by V' (we keep in this subgraph with vertex set V' all the edges of G with both endpoints in
 147 V').

148 A *triangle* in a graph is a C_3 , a cycle of length three. A graph is *planar* if it can be drawn
 149 in the 2-dimensional plane so that no two edges meet in a point other than a common end.
 150 A triangle of a plane graph is a *facial triangle* if the triangle is the boundary of a face of the
 151 plane graph. We call a face of a plane graph a *triangular face* if its boundary is a triangle.

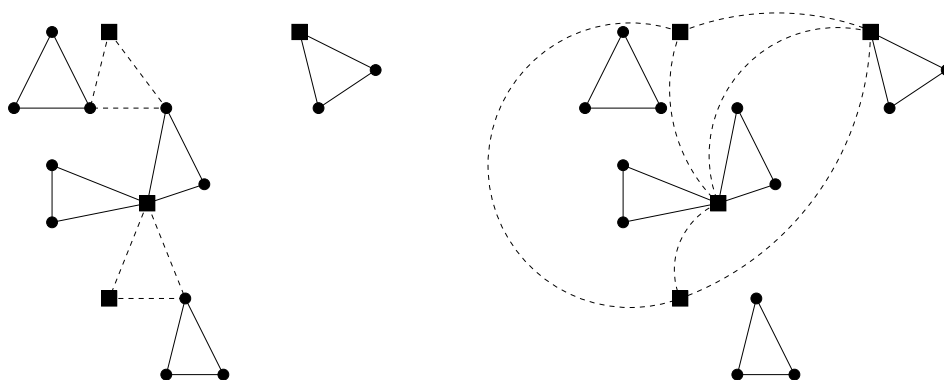
152 A *cut-vertex* (respectively, *bridge*) is a vertex (resp., edge) whose deletion increases the
 153 number of components. A graph is said to be a *biconnected graph*, if it has at least three
 154 vertices and it does not contain any cut-vertices. A *block* is a maximal connected subgraph
 155 without a cut-vertex. Thus, every block is either a maximal biconnected subgraph, or a
 156 bridge.

157 Graphic Matroid Parity is the following problem: given a multigraph $G' = (V', E')$ and a
 158 partition of the edge set E' into pairs of distinct edges $\{f, f'\}$, find a (simple) forest $F \subseteq E'$
 159 with the maximum number of edges, such that $f \in F$ if and only if $f' \in F$, for all $f \in E'$.

160 Graphic Matroid Parity algorithms can be used to construct a maximum triangular cactus
 161 in a given graph [25]. Indeed, given a graph $G = (V, E)$, one constructs G' by having $V' = V$,
 162 and for each triangle T of G , let e, e' be any pair of distinct edges in T . Add two new edges
 163 f and f' to E' , f with the same endpoints as e , and f' with the same endpoints as e' . Pair
 164 f with f' in the partition of E' . The straightforward lemma 2.13 of [5] states that a forest F
 165 of G' as above with $2p$ edges exists if and only if a triangular cactus with p triangles exists
 166 in G .

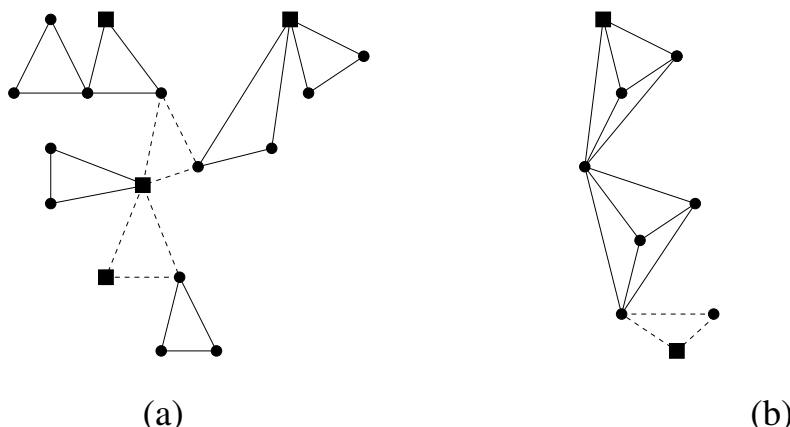
167 **3** Local Optimization after Max Triangular Cactus

168 Here is our first approximation algorithm, Algorithm **MTLK4**: Start with a maximum
 169 triangular cactus. As long as possible, if there exists a K_4 in the input graph and at most
 170 two edge-disjoint triangles in our kt-structure such that removing the (one or two) triangles
 171 and adding the K_4 results in a kt-structure, do this replacement. See figures 3 and 4 for
 172 illustrations. Each such replacement increases the cyclomatic number¹⁰ of the kt-structure,
 173 and thus this is a polynomial-time algorithm. Precisely, there are $O(n^4)$ K_4 's to consider and
 174 for each we can look at $O(n^2)$ ways to choose two existing triangles for replacement (these
 175 two triangles come from a graph with $O(n)$ edges). So we can achieve each replacement in
 176 $O(n^7)$ time, for a total running time, excluding the Matroid Parity algorithm, of $O(n^8)$.



■ **Figure 3** On the left side, the current kt-structure, with two connected components. There is a K_4 in the input graph, with its four vertices represented by small filled squares. Two triangles from the current kt-structure, dashed, can be removed to disconnect these four vertices, after which the K_4 (with edges represented by dashed cycle arcs) can be added resulting in another kt-structure (on the right side, with three connected components) with a higher cyclomatic number.

¹⁰The cyclomatic number (also called circuit rank, cycle rank, or nullity) of an undirected graph is the minimum number of edges that must be removed from the graph to break all its cycles, making it into a tree or forest.



■ **Figure 4** Both (a) and (b) show kt-structures where, for each of them, two triangles (dashed) can be removed to allow a K_4 , whose vertices are represented by small filled squares, to be added resulting in a kt-structure.

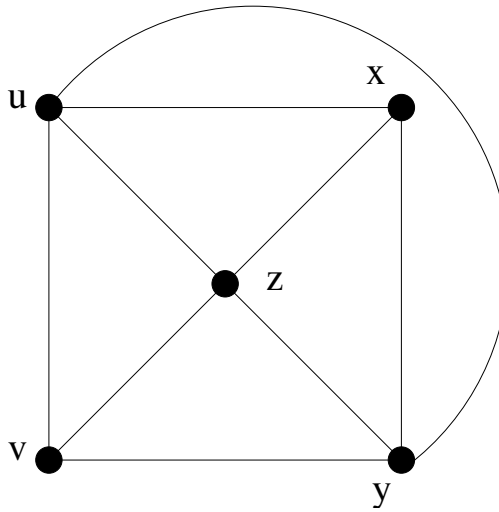
177 We believe that an $O(n^5)$ -running time version of the algorithm exists, based on the
 178 following idea. One needs to read the proof of the approximation ratio first, as we modify
 179 the algorithm. We only check for each K_4 if there is no strong bond, and its four vertices
 180 are not all in the same component of the current kt-structure. This check can be done in
 181 $O(1)$ after computing connected components by Depth First Search (and this has to be done
 182 only once after each local improvement). A K_4 that does not pass this check is not used for
 183 the local improvement, even though in MTLK4 it could possibly lead to improvement (see
 184 Figure 4 (a)). However, we cannot get a $O(n^4)$ running time by showing that a K_4 that was
 185 found not useful once will not become useful in the future. We have a counterexample.

186 The rest of the section will be spent on the approximation ratio analysis.

187 **First, some intuition.** Let $\beta(\bar{G})$ be the number of triangles in a maximum triangular
 188 cactus in graph \bar{G} . It is known from [5] (see also Inequality (2) below) that, if \tilde{H} is a planar
 189 graph on n vertices with $|E(\tilde{H})| = 3n - 6 - t$, then $\beta(\tilde{H}) \geq (1/3)(n - t - 2)$. With G the input
 190 graph and H an optimum solution (a maximum planar subgraph of G), we obtain that the
 191 output of the MT algorithm (which, recall, computes the triangular cactus with maximum
 192 number of triangles, and then connects the components of this cactus) has $n - 1 + \beta(G)$
 193 edges (since every triangle gains one edge over a spanning tree), and we obtain a ratio of
 194 $4/9$ from $\beta(G) \geq \beta(H)$. With θ such that H has $3n - 6 - \theta$ edges, from simple algebraic
 195 manipulation, we would have an $\epsilon > 0$ improvement over $4/9$ if $\theta \geq \epsilon' n$ for some $\epsilon' > 0$. But
 196 we cannot count on this happening.

197 So now we assume that θ is close to 0. As we use K_4 's, the second question is what happens
 198 if H (the optimum solution as above) does not have any K_4 's. The bound $\beta(H) \geq (1/3)(n -$
 199 $\theta - 2)$ is not tight anymore, and in fact with $\theta = 0$ we are able to prove that $\beta(H) \geq (3/7)n - 1$
 200 when H has no K_4 's. This is good as $(n + (3/7)n - 2)/(3n - 6) \geq 10/21 > 4/9$.

201 So we assume that θ is close to 0 and H has K_4 's. To quantify the benefits of these K_4 's,
 202 we introduce some notation (see Figure 5 for an illustration):



■ **Figure 5** In this triangulated plane graph, x and v are the cubic (degree three) vertices.

203 ► **Definition 1.** Call a vertex v of a triangulated plane graph \tilde{H} cubic if it has degree three
 204 (so we have a K_4 formed by v and its neighbors). Let $c(\tilde{H})$ be the number of cubic vertices
 205 in \tilde{H} .

206 Theorem 5 below obtains that $\beta(\tilde{H}) \geq (3/7)n - (1/7)c(\tilde{H}) - 1$, with $n = |V(\tilde{H})|$. With
 207 \tilde{H} a triangulated supergraph of H on the same vertex set, we have that \tilde{H} contains exactly
 208 θ edges not in H . Then we can obtain that $\beta(H) \geq (3/7)n - (1/7)c(\tilde{H}) - 1 - \theta$. Now, if
 209 $c(\tilde{H})$ is also small in addition to θ being close to 0, we have again a ratio bigger than 4/9.
 210 And when $c(\tilde{H})$ is “large” compared to n , and θ is close to 0, then there are enough K_4 ’s in
 211 H for the local optimization phase of MTLK4 to use, as shown after Theorem 5. We are
 212 done with providing some intuition. As small graphs are easy to handle, we assume that
 213 $n = |V(G)| > 4$ in this section. On our way to Theorem 5 we need a lot of notation.

214 **Double-partitions.** Let $\bar{G} = (V, E)$ be a graph on n vertices. Let $\mathcal{P} = \{V_1, \dots, V_k\}$ be
 215 a partition of the vertices of \bar{G} into *vertex classes*, and $\mathcal{Q} = \{E_1, \dots, E_q\}$ be a partition of
 216 the edges of \bar{G} into *edge colors*. We say that an edge color and a vertex class are incident if
 217 at least one of the edges of the edge color is incident to at least one of the vertices of the
 218 vertex class. For $1 \leq i \leq q$, let u_i denote the number of vertex classes V_j of \mathcal{P} incident to
 219 edge color E_i of \mathcal{Q} . We say that “double-partition” $(\mathcal{P}, \mathcal{Q})$ covers a triangle if the triangle
 220 has at least two vertices in the same vertex class of \mathcal{P} (when we also say that the triangle is
 221 covered by this vertex class) or all three edges in the same edge color of \mathcal{Q} (when we also say
 222 that the triangle is covered by this edge color). We call the double-partition $(\mathcal{P}, \mathcal{Q})$ valid for
 223 \bar{G} if every triangle of \bar{G} is covered. Set¹¹:

$$224 \quad \Phi(\mathcal{P}, \mathcal{Q}) = n - k + \sum_{i=1}^m \lfloor \frac{u_i - 1}{2} \rfloor. \tag{1}$$

225 Since $k \leq n$ and $u_i \geq 1$ for all i , we have that $\Phi(\mathcal{P}, \mathcal{Q}) \geq 0$, and note that there is always a
 226 valid double-partition $(\mathcal{P}, \mathcal{Q})$ for \bar{G} (e.g., $k = 1$ and $q = 1$ and $V_1 = V(\bar{G})$ and $E_1 = E(\bar{G})$).

¹¹The formula given here, which differs from that in [25] by having floors, is correct. See also [30] or Theorem 11.3.2 of [25].

227 Call a vertex class a *trivial vertex class* if it has just one vertex, call this vertex a *singleton*,
 228 and an edge color a *trivial edge color* if it has just one edge. The *contribution* of an edge
 229 color E_i of \mathcal{Q} to $\Phi(\mathcal{P}, \mathcal{Q})$ is the quantity $\lfloor \frac{u_i-1}{2} \rfloor$. The *contribution* of \mathcal{P} to Φ is defined to be
 230 $n - k$.

231 According to Lovász and Plummer [25], we have:

232 ► **Proposition 2** (Theorem 11.3.6 in [25]). *The number of triangles in a maximum triangular*
 233 *cactus in a graph \tilde{G} is equal to the minimum of $\Phi(\mathcal{P}, \mathcal{Q})$ taken over all valid double-partitions*
 234 *$(\mathcal{P}, \mathcal{Q})$ for \tilde{G} .*

235 Let \tilde{H} be a planar graph with $n \geq 3$ vertices. Embed \tilde{H} in the plane without crossing
 236 edges, obtaining a plane graph. Let t be the number of edges *missing* for this embedding to
 237 be triangulated (meaning that adding t edges to \tilde{H} would result in a triangulated planar
 238 graph). A triangulated plane graph has $3n - 6$ edges, if $n \geq 3$. So $t = (3n - 6) - |E(\tilde{H})|$; t
 239 does not depend on the embedding. The 4/9-approximation of [5] is based on:

240 ► **Proposition 3** (Theorem 2.3 of [5], also equivalent to Corollary 1.2 of [8]). *Let \tilde{H} be a*
 241 *connected planar graph with $n \geq 3$ vertices. Let t be the number of missing edges, defined as*
 242 *above. Then*

$$243 \quad \Phi(\mathcal{P}, \mathcal{Q}) \geq \frac{1}{3}(n - 2 - t),$$

244 *for all valid double-partitions $(\mathcal{P}, \mathcal{Q})$ for \tilde{H} .*

245 This bound is known to be asymptotically tight when $t = 0$, see for example [5] where
 246 their 4/9-approximation is proven tight. Recall that $\beta(\tilde{H})$ is the number of triangles in a
 247 maximum triangular cactus in \tilde{H} . From Propositions 2 and 3 we obtain:

$$248 \quad \beta(\tilde{H}) \geq \frac{1}{3}(n - 2 - t), \tag{2}$$

249 If a double-partition $(\mathcal{P}, \mathcal{Q})$ is valid for plane graph \tilde{H} , then it must cover all the facial
 250 triangles of \tilde{H} .

251 ► **Definition 4.** *Call a double-partition $(\mathcal{P}, \mathcal{Q})$ of a plane graph \tilde{H} p-valid if it covers the*
 252 *facial triangles of \tilde{H} .*

253 Note that a valid double-partition $(\mathcal{P}, \mathcal{Q})$ of a graph \tilde{G} is p-valid for any plane embedding
 254 of \tilde{G} . The main technical result of this section is Theorem 5 below, which gives a lower
 255 bound for $\Phi(\mathcal{P}, \mathcal{Q})$ for all p-valid double partitions $(\mathcal{P}, \mathcal{Q})$ of a triangulated plane graph \tilde{H}
 256 in terms of n and $c(\tilde{H})$. The accounting part of the lower bound is proven assuming that
 257 the double partition $(\mathcal{P}, \mathcal{Q})$ satisfies a number of conditions. Ideally, we would want that \mathcal{P}
 258 would have only one vertex class P_1 with more than one vertex (we are not able to ensure
 259 this condition); this condition would make the accounting much simpler.

260 We will enumerate the actual conditions later. To get that $(\mathcal{P}, \mathcal{Q})$ satisfy these actual
 261 conditions, we *modify* $(\mathcal{P}, \mathcal{Q})$, which really means obtaining from a p-valid $(\mathcal{P}, \mathcal{Q})$ another
 262 double partition $(\mathcal{P}', \mathcal{Q}')$ such that $\Phi(\mathcal{P}, \mathcal{Q}) \geq \Phi(\mathcal{P}', \mathcal{Q}')$ and such that $(\mathcal{P}', \mathcal{Q}')$ is also p-valid
 263 for \tilde{H} . It is fine to make such modifications since, once we prove a lower bound for $(\mathcal{P}', \mathcal{Q}')$,
 264 then it holds for $(\mathcal{P}, \mathcal{Q})$ as well.

265 Assuming that \tilde{H} is a triangulated plane graph, one can easily verify based on the
 266 definition of $\Phi(\mathcal{P}, \mathcal{Q})$ (Equation (1)) that we can do the following **modifications**:

3:10 Local Optimization Algorithms for Maximum Planar Subgraph

- 267 1. Any edge of \tilde{H} such that both facial triangles that contain this edge are covered by vertex
 268 classes is put into an edge color by itself (we can do this since this trivial edge color
 269 contributes 0 to Φ , and the contribution of any other edge color does not increase). In
 270 particular, any edge that is incident to two vertices in the same vertex class is put into
 271 an edge color by itself.
- 272 2. If we have two distinct edge colors both incident to the same two (or more) distinct vertex
 273 classes, these two edge colors can be merged into one edge color.
- 274 3. If an edge color Q_i can be partitioned into two edge colors Q' and Q'' such that all the
 275 facial triangles covered by Q_i are covered by Q' or Q'' , and Q' and Q'' are incident to at
 276 most one common neighbor among the vertex classes, split Q_i into Q' and Q'' .

277 Recall Definition 1. One main technical result is:

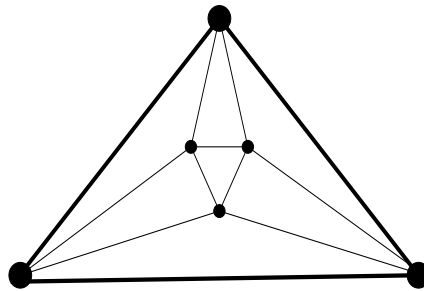
278 ► **Theorem 5.** *Let \tilde{H} be a triangulated plane graph with $n \geq 3$ vertices, and let $(\mathcal{P}, \mathcal{Q})$ be a*
 279 *double-partition p -valid for \tilde{H} . Then:*

$$280 \quad \Phi(\mathcal{P}, \mathcal{Q}) \geq \frac{3}{7}n - \frac{1}{7}c(\tilde{H}) - 1. \quad (3)$$

281

282 This very long proof appears later. We give some shorter intuition now. Equation (3) is
 283 tight (excluding a small additive term), as shown by the following two constructions. Both of
 284 them provide useful examples for the intuition behind the proof. Below, we use c to denote
 285 the number of cubic vertices of the plane graph being discussed. Consider a triangulation W
 286 on r vertices containing no K_4 . From Euler's formula we get that W has $2r - 4$ faces. In
 287 the first construction, insert one cubic vertex in every face. We have $n = r + (2r - 4)$ and
 288 $c = 2r - 4$. We take \mathcal{P} to have only one non-trivial vertex class, W , and \mathcal{Q} to have only
 289 trivial edge colors; note that the double partition $(\mathcal{P}, \mathcal{Q})$ is p -valid for the constructed plane
 290 graph. Thus $\Phi(\mathcal{P}, \mathcal{Q}) = r - 1 = (3/7)n - (1/7)c - (1/7)$.

291 In the second construction, insert three new vertices into every face of W as in Figure 6.
 292 We have $n = r + 3(2r - 4) = 7r - 12$ and $c = 0$. We take \mathcal{P} to have only one non-trivial
 293 vertex class, W , and \mathcal{Q} to have $2r - 4$ non-trivial edge colors, each with the edges embedded
 294 strictly in each face of W . Each of these non-trivial edge colors is incident to exactly 4 vertex
 295 classes: the three singletons (singletons are vertices) inside the face of W , and the non-trivial
 296 class comprised of W . Thus $\Phi(\mathcal{P}, \mathcal{Q}) = r - 1 + 2r - 4 = (3/7)n + (1/7)$. Also note that the
 297 double partition $(\mathcal{P}, \mathcal{Q})$ is p -valid for the constructed plane graph.



■ **Figure 6** A face of W is shown in solid edges.

298 **Intuition.** To show some of the proof ideas, we make the simplifying assumption that \mathcal{P}
 299 has only one non-trivial part, which we call R (we could not find a way to enforce this

300 assumption and ended up with a much longer proof). We also make another two simplifying
 301 assumptions, that $r := |R| > 2$ and that $\tilde{H}[R]$ is a connected graph (Removing these two
 302 assumptions seems possible with some effort). First, apply Modification 1 such that any edge
 303 of $\tilde{H}[R]$ is put into an edge color by itself.

304 For a face F of $\tilde{H}[R]$, call S_F the set of singletons embedded strictly inside F . We discuss
 305 now the case $|S_F| > 1$. Due to \tilde{H} being triangulated, $\tilde{H}[S_F]$ is connected. Walking around
 306 $s \in S_F$ in clockwise manner, we get a circular list L of vertices that are not all in the same
 307 vertex class. When we switch in L from one class to another, we have one facial triangle T_1
 308 of \tilde{H} that is not covered by a vertex class. Later in the walk, when again we switch in L
 309 from one vertex class to another, we have another facial triangle T_2 of \tilde{H} that is not covered
 310 by a vertex class. If there are two distinct edge colors Q_1 and Q_2 of \mathcal{Q} covering T_1 and T_2 ,
 311 then there are two distinct vertex classes incident to both Q_1 and Q_2 and we can apply
 312 Modification 2. Continue this traversal of L and get that all the facial triangles incident
 313 to s that are not covered by R are covered by one single edge color. $\tilde{H}[S_F]$ is connected,
 314 and we can do a depth-first search traversal and as we meet the vertices of S_F , we do the
 315 walk-around described above for each of them to obtain that all the facial triangles of \tilde{H}
 316 embedded in F that are not covered by R are covered by one single edge color which we call
 317 Q_F . By construction, Q_F meets all the singletons of S_F and the vertex class R .

318 If edge color Q_F as above also covers facial triangles outside F , then we can apply
 319 Modification 3, where Q' consist of the edges of Q_F embedded strictly inside F and Q''
 320 consists of the other edges of Q_F ; note that only R among the vertex classes can be incident
 321 to both Q' and Q'' . After doing this for all the faces of $\tilde{H}[R]$, we get that any non-trivial
 322 edge color is the Q_F for some face F with $|S_F| > 1$ of $\tilde{H}[R]$, and all the edges of Q_F are
 323 embedded strictly inside F . Note that when $|S_F| = 0$ or $|S_F| = 1$, all the triangular faces
 324 of \tilde{H} embedded in F are covered by R . And all the triangular faces of \tilde{H} are embedded in
 325 some face F of $\tilde{H}[R]$. We now have:

$$326 \quad \Phi(\mathcal{P}, \mathcal{Q}) = (r - 1) + \sum_{F \text{ face of } \tilde{H}[R]} \lfloor |S_F|/2 \rfloor = (r - 1) + \sum_{i \geq 0} f_i \lfloor \frac{i}{2} \rfloor, \quad (4)$$

327 where f_i is the number of faces of $\tilde{H}[R]$ each with i singletons embedded inside. Let c_1 be
 328 the number of triangular faces of $\tilde{H}[R]$ with exactly one singleton embedded inside. As any
 329 such singleton is a cubic vertex,

$$330 \quad c_1 \leq c. \quad (5)$$

331 Let d_1 be the number of non-triangular faces of $\tilde{H}[R]$ with one singleton inside, so that

$$332 \quad f_1 = c_1 + d_1. \quad (6)$$

333 We would have $2r - 4$ triangular faces of $\tilde{H}[R]$ if it were triangulated. A non-triangulated
 334 face can be replaced by two or more triangulated faces by adding "fake" edges, and thus
 335 from which we deduce:

$$336 \quad 2r \geq c_1 + 2d_1 + f_3 + f_5, \quad (7)$$

337 and therefore

$$338 \quad 4r \geq 2c_1 + 4d_1 + 2f_3 + 2f_5 \geq 2c_1 + 3d_1 + 2f_3 + f_5. \quad (8)$$

339 Using the equation above, Equation (6), and Equation (5) we obtain:

$$340 \quad \frac{4}{7}r \geq \frac{2}{7}c_1 + \frac{3}{7}d_1 + \frac{2}{7}f_3 + \frac{1}{7}f_5 = \frac{3}{7}f_1 + \frac{2}{7}f_3 + \frac{1}{7}f_5 - \frac{1}{7}c_1 \geq \frac{3}{7}f_1 + \frac{2}{7}f_3 + \frac{1}{7}f_5 - \frac{1}{7}c.$$

3:12 Local Optimization Algorithms for Maximum Planar Subgraph

341 For $i \in \{0, 2, 4, 6, 7, 8, 9, \dots\}$, we have $\lfloor i/2 \rfloor \geq \frac{3}{7}i$. Using this, the equation above,
 342 Equation (4), and $n = |V(\tilde{H})| = r + \sum_{i \geq 0} i \cdot f_i$, we obtain:

$$343 \quad \Phi(\mathcal{P}, \mathcal{Q}) = (r - 1) + \sum_{i \geq 0} f_i \lfloor \frac{i}{2} \rfloor \geq \frac{3}{7}(r + \sum_{i \geq 0} i \cdot f_i) - \frac{1}{7}c - 1 = \frac{3}{7}n - \frac{1}{7}c - 1,$$

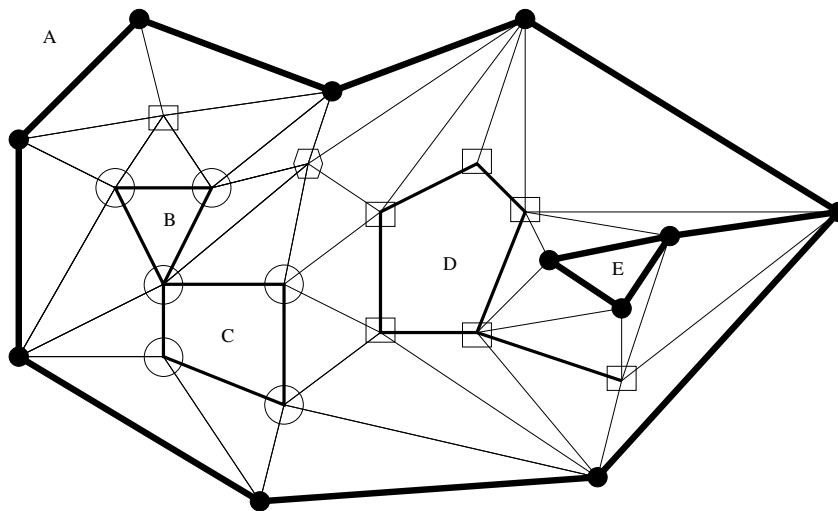
344 or Equation (3). We are done providing intuition for the proof of Theorem 5.

345 **Proof.** (of Theorem 5) This long proof has two stages: first stage modifies (if needed) the
 346 double-partition $(\mathcal{P}, \mathcal{Q})$ so that it satisfies five conditions, and the second stage does the
 347 accounting using the five conditions. A number of definitions are needed before the first
 348 stage starts.

349 We use c to denote $c(\tilde{H})$ and Φ to denote $\Phi(\mathcal{P}, \mathcal{Q})$. Let P_1, P_2, \dots, P_h be the non-trivial
 350 vertex classes of \mathcal{P} , and let $p_i = |P_i|$.

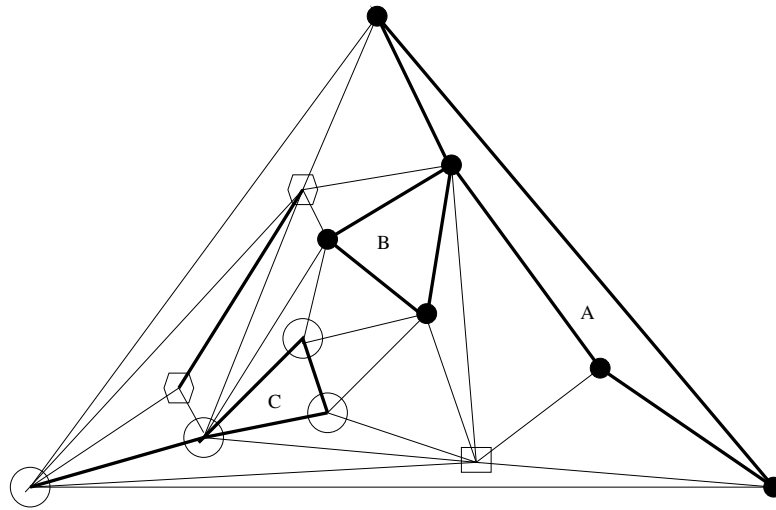
351 Define $B_i := \tilde{H}[P_i]$, and let B_i 's connected components be $B_i^1, B_i^2, \dots, B_i^{j_i}$. Note that if
 352 a vertex class covers a facial triangle, then there exists an i with B_i containing an edge e of
 353 the triangle. If this happens we say that e *v-covers* the facial triangle.

354 Let B_i^j be some component of some B_i and let F be an inner face of B_i^j that contains at
 355 least one vertex of \tilde{H} . Let $L_i^j(F)$ be the border of F ($L_i^j(F)$ is a subgraph of B_i^j). Consider
 356 all the vertices v and edges e embedded in F but not embedded strictly inside any face F'
 357 of some $B_{i'}^{j'}$ such that F' is included in F . These vertices and edges plus $L_i^j(F)$ comprise a
 358 plane subgraph of \tilde{H} that we call an *internal soup*. $L_i^j(F)$ is called the *main border* of the
 359 internal soup. See Figure 7 for an example. Call F (as a region of the plane) the *territory* of
 360 the internal soup. Define a *relevant facial triangle* of an internal soup to be a facial triangle
 361 whose three vertices belong to more than one vertex class (equivalently, these three vertices
 362 are not in the same B_i).



■ **Figure 7** An example of an internal soup. The edges and vertices strictly inside the faces A, B, C, D, and E are not part of the soup. There are four vertex classes here, depicted by circles, squares, filled circles, and hexagons. Here, the vertex class depicted by squares is not connected. The main border of this soup is represented by very thick segments. Thick segments represent other edges with both endpoints in the same vertex class. Thin segments represent edges of the soup with endpoints in different vertex classes. All the depicted triangles except possibly B and E are facial triangles of \tilde{H} . The territory of this soup is the plane without the interior of the face A. There are 33 relevant facial triangles of this soup — they all have at least one thin edge. If B or E are facial triangles of \tilde{H} , they are not relevant facial triangles of the soup.

363 Let u, v, w be the three vertices on the border of the outer face of \tilde{H} . If u, v, w are not
 364 contained in the same B_i , for some i , we also have an *external soup* defined as above using
 365 as F (in the definition) the region of the plane that is the complement of the outer face of \tilde{H} .
 366 The external soup does not have a main border. The territory of the external soup is defined
 367 to be the region of the plane that is the complement of the outer face of \tilde{H} . See Figure 8 for
 368 an example.



■ **Figure 8** An example of an external soup. Here F is the region of the plane that is the complement of the outer face of \tilde{H} (unlike internal soups, and despite its name, here F is not a face of some B_i^j). The edges and vertices strictly inside the faces A, B, and C, are not part of the soup. There are four vertex classes here, depicted by circles, squares, filled circles, and hexagons. Thick segments represent edges with both endpoints in the same vertex class. Thin segments represent edges of the soup with endpoints in different vertex classes. All the depicted triangles except possibly B and C are facial triangles of this soup — they all have at least one thin edge and include the facial triangle of the outer face of \tilde{H} . If B or C are facial triangles of \tilde{H} , they are not relevant facial triangles of the soup.

369 Note that every facial triangle of \tilde{H} is either a facial triangle of some soup, or has all its
 370 three edges in some B_i (and vertex class P_i v -covers the facial triangle).

371 We say that a component B_i^j *participates* in a soup D if B_i^j does not contain the main
 372 border of the soup D and at least one vertex of B_i^j is a vertex of the soup. Recall that a
 373 singleton is a vertex that belongs to a size 1 vertex class. Singletons that are part of the
 374 soup also *participate* in the soup. For example, in Figure 7, we have three components and a
 375 singleton that participate in the depicted soup (this is since the vertex class represented by
 376 squares has two components that participate in the soup).

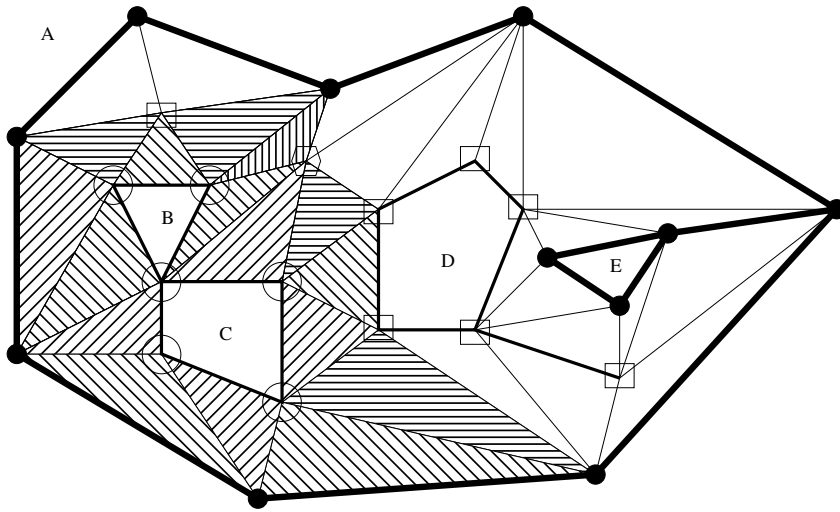
377 Later, the proof requires that the double-partition $(\mathcal{Q}, \mathcal{P})$ satisfies the following **five**
 378 **conditions** (goals):

- 379 1. Any edge of \tilde{H} such that both facial triangles that contain this edge are covered by vertex
 380 classes is in an edge color by itself. In particular, any edge that is incident to two vertices
 381 in the same vertex class is in an edge color by itself;
- 382 2. At most one edge color covers facial triangles in a soup;
- 383 3. Each B_i is connected (recall that $B_i = \tilde{H}[P_i]$, where P_i is a vertex class of \mathcal{P});
- 384 4. An edge color covers facial triangles in at most one soup;
- 385 5. There is no i with $|P_i| = 2$.

386 We start the **first stage** now, working towards these goals. All the relevant facial triangles
 387 in a soup must be covered by double-partition $(\mathcal{P}, \mathcal{Q})$, so any relevant facial triangle is covered
 388 by either one vertex class of \mathcal{P} or by an edge color of \mathcal{Q} . Apply Modification 1 to $(\mathcal{P}, \mathcal{Q})$,
 389 so that any edge of \tilde{H} such that both facial triangles that contain this edge are covered by
 390 vertex classes is put into an edge color by itself, achieving our *first goal*. In particular, any
 391 edge of \tilde{H} connecting two vertices in the same vertex class is put into an edge color by itself.

392 Now every relevant facial triangle of every soup is covered either by a vertex class or by an
 393 edge color but not both.

394 Next we modify, if needed, $(\mathcal{P}, \mathcal{Q})$, so that at most one edge color is used for covering all
 395 the relevant facial triangles in a soup that are not covered by a vertex class. If this is not the
 396 case, we use Modification 2, as described below. That we can do this relies on topological
 397 arguments. Let $L_i^j(D)$ be the outer border of some component B_i^j that participates in a
 398 soup D . As we walk clockwise on $L_i^j(D)$, we encounter relevant facial triangles of the soup,
 399 some with one edge in $L_i^j(D)$, and others with only one vertex in $L_i^j(D)$. These relevant
 400 facial triangles form the *moat* of B_i^j in D . See Figure 9 for an illustration. Similarly, we
 401 define the *moat* of a singleton w to consist of all the relevant facial triangles that contain
 402 w . A moat of a component B_i^j (or a singleton) that participates in the external soup can
 403 include the outer face of \tilde{H} .



■ **Figure 9** An example of a moat, inside the soup represented in Figure 7. The facial triangles (and corresponding triangular faces) with patterns illustrate the moat of the connected component of the vertex class whose vertices are marked by empty circles. The pattern is diagonal if the facial triangle is covered by a vertex class, and horizontal or vertical if the facial triangle must be covered by an edge color.

404 If on the outer border of a moat in an internal soup D we only have vertices from the
 405 main border of D , one can easily check that all the soup D consists of this moat, and all the
 406 relevant facial triangles in the soup D are covered by vertex classes. For an external soup D ,
 407 if on the outer border of a moat we only have vertices from some a single $L_{i'}^{j'}(D)$ or a single
 408 singleton, one can easily check that all the soup D consists of this moat, and all the relevant
 409 facial triangles in the soup D are covered by vertex classes. If not, as we walk on the outer
 410 border of the moat, when we switch from some $L_{i'}^{j'}(D)$ to another (or to a singleton or to
 411 the main border, or from a singleton to another or to some $L_{i'}^{j'}(D)$ or to the main border, or
 412 from the main border to a singleton or to some $L_{i'}^{j'}(D)$), we have a relevant facial triangle T_1
 413 that has its three vertices in three different vertex classes and therefore must be covered by
 414 an edge color. And later in the walk we have another facial triangle T_2 that must be covered
 415 by an edge color (when we switch the vertex class outside the moat, as in Figure 9). If there
 416 are two distinct edge colors Q_1 and Q_2 of \mathcal{Q} covering T_1 and T_2 , then there are two distinct
 417 vertex classes incident to both Q_1 and Q_2 and we can apply Modification 2. Continue around
 418 this moat and other moats in the soup D , until we get that all the relevant facial triangles in

419 the soup D that are not covered by vertex classes are covered by the same edge color. This
 420 continuation works since \tilde{H} is triangulated and thus all the moats of a soup are “connected”
 421 as they overlap. More precisely, we treat two moats as being adjacent if they share a relevant
 422 facial triangle, and then one can easily check that the space of moats of a soup is connected,
 423 allowing us to obtain that every relevant facial triangle in the soup that is covered by an
 424 edge color is covered by the same edge color.

425 The changes done here do not invalidate the first goal, and do not change any of the
 426 soups. Thus from now on $(\mathcal{P}, \mathcal{Q})$ satisfies that at most one edge color is used for covering all
 427 the relevant facial triangles in a soup not covered by vertex classes, achieving our *second goal*.

428 Our *third goal* is to modify the double-partition $(\mathcal{P}, \mathcal{Q})$ to obtain that each B_i is connected.
 429 We also want that each non-trivial edge color covers relevant facial triangles in only one soup
 430 (*fourth goal*). Recall that P_i 's are the parts of \mathcal{P} and that $B_i := \tilde{H}[P_i]$, and B_i 's connected
 431 components are $B_i^1, B_i^2, \dots, B_i^{j_i}$.

432 The soups of \tilde{H} can be arranged to be the vertices of a forest \mathcal{F} , by containment of their
 433 territories: if the territory of soup D is inside the territory of soup D' , then D is a descendant
 434 of D' . If an external soup exists, \mathcal{F} is a tree with the external soup as the root. Leaves
 435 of \mathcal{F} are the soups whose territory does not contain the territory of any other soup. We
 436 traverse \mathcal{F} in postorder, keeping the **invariant** that, when processing soup D , all the soups
 437 D' descendants of D satisfy the following property: All the B_i^j embedded in the territory
 438 of D' , except possibly for the B_i^j that contains the main border of D' , are in fact a B_i (in
 439 other words, B_i is connected), the edge color that covers relevant facial triangles of D' , if
 440 any, has all of its edges in D' , and the first two goals are also achieved. We now work on D
 441 to obtain the same properties and maintain the invariant during this postorder proposal.

442 As above, $L_i^j(D)$ denotes the border of some B_i^j as it participates in a soup D (by the
 443 definition of “participate”, $L_i^j(D)$ is not the main border of D). We have (from the second
 444 goal) that at most one edge color covers relevant facial triangles in the soup D . If B_i has
 445 some components other than B_i^j , we modify \mathcal{P} by splitting the vertex class P_i into two vertex
 446 classes, one consisting of the vertices of $V(B_i^j)$ and the other consisting of $P_i \setminus V(B_i^j)$. All the
 447 facial triangles are still covered by the new double-partition, since a facial triangle T covered
 448 before the modification by the vertex class P_i must be v-covered before the modification by
 449 an edge of B_i and this edge would be in either B_i^j or in what is left from B_i after removing
 450 $V(B_i^j)$ from B_i , thus v-covering after the modification the facial triangle T . We claim that
 451 Φ does not go up: the contribution of \mathcal{P} decreases by 1, while the total contribution of edge
 452 colors increases by at most 1, since trivial edge colors contribute 0 to Φ , and only the (single)
 453 non-trivial edge color, which we call Q_i , that contains edges in the soup D can have its u_i
 454 incremented (recall that u_i is the number of vertex classes incident to Q_i). Indeed, other
 455 non-trivial edge colors that are incident to the new vertex class that consists of $V(B_i^j)$ can
 456 only cover relevant facial triangles of soups with territory included in interior faces of B_i^j ,
 457 and these edge colors are not incident to any $B_i^{j'}$, for $j' \neq j$, from the invariant. After we
 458 apply this step to all the B_i^j participating in the soup D , except for the main border of the
 459 soup D , we do have that all such B_i^j are in fact a B_i .

460 If there exists an edge color Q covering relevant facial triangles of D and Q also covers
 461 facial triangles elsewhere, apply Modification 3 and split Q into Q' and \bar{Q} , where Q' consist
 462 of the edges of Q inside the soup D . Note that the edges of \bar{Q} are embedded outside the
 463 territory of D , from the invariant. All the facial triangles covered by Q are now covered by
 464 either Q' or \bar{Q} ; this is since the facial triangles that have one edge in the main border of D
 465 are not covered by an edge color (from the first goal). Also, there is at most one vertex class,
 466 (specifically, the P_i that contains the vertices of the main border of D) that is incident to

467 both Q' and \bar{Q} , since the edges of \bar{Q} are embedded outside the territory of D and all the
 468 vertex classes $P_{i'}$ that have vertices inside the territory of D , except for the P_i that contains
 469 the vertices of the main border of D , form a connected $B_{i'}$ (from the invariant) and hence
 470 $P_{i'}$ cannot have vertices outside the territory of D .

471 Note that none of the changes invalidate the first two goals, or modify the soups. By now,
 472 we achieved our first four goals: any edge of \tilde{H} such that both facial triangles that contain
 473 this edge are covered by vertex classes is in an edge color by itself (in particular any edge of
 474 \tilde{H} connecting two vertices in the same vertex class is in an edge color by itself), at most one
 475 edge color covers facial triangles in a soup, double-partition $(\mathcal{P}, \mathcal{Q})$ has each B_i connected,
 476 and each non-trivial edge color covers facial triangles in only one soup. Moreover, the facial
 477 triangles in a soup that are not covered by vertex classes, if they exist, are all covered by one
 478 single edge color.

479 We further modify the double-partition $(\mathcal{P}, \mathcal{Q})$, to have that $|P_i| \neq 2$, for all i . Let us
 480 look at one P_i with $|P_i| = 2$. The graph B_i is connected by now, so let us look at the soup
 481 D where B_i participates (B_i cannot contain the main border of a soup), and at the moat
 482 around B_i . In a first case, the outer border of this moat is the main border of the soup D .
 483 Then all facial triangles of the soup D are covered by vertex classes. We split the vertex class
 484 P_i into two singleton vertex classes, and put all the edges of D into a new edge color thus
 485 covering the two facial triangles that B_i used to cover. Then we apply Modification 1. The
 486 contribution of \mathcal{P} to Φ decreased by 1, while the contribution of this new edge color is exactly
 487 1 (it is incident to exactly three vertex classes). Note that this modification does not destroy
 488 any of our first four goals. In a second case, the moat around B_i has two or more vertex
 489 classes on its outer border. Then there is one edge color that covers facial triangles in the
 490 soup D . In particular, this edge color is incident to P_i as it covers at least one facial triangle
 491 with (exactly) one vertex in P_i . Once again split the vertex class P_i into two singleton vertex
 492 classes, and put all the edges incident to P_i in the edge color that covers facial triangles in
 493 the soup D , thus covering the two facial triangles that B_i used to cover. Then we apply
 494 Modification 1. Once again, the contribution of \mathcal{P} to Φ decreased by 1, while in this second
 495 case the contribution of this edge color covering relevant facial triangles in D increased by at
 496 most 1, as it is incident to one more vertex class. The contribution of other edge colors does
 497 not change. Note that this modification does not destroy any of our first four goals and does
 498 not modify the soups.

499 We have finished the first stage of the proof, and by now the double-partition $(\mathcal{Q}, \mathcal{P})$
 500 satisfies the five conditions.

501 We continue with the **second stage** of the proof. Fix D to be a soup which meets
 502 g vertex classes. These g vertex classes give raise to the components or singletons that
 503 participate in the soup, and to the main border of the soup if the soup is an internal soup.
 504 Each of these vertex classes is connected in \tilde{H} and also its intersection with the soup is
 505 connected.

506 \triangleright **Claim 6.** Exactly $2g - 4$ relevant facial triangles of the soup D are not covered by vertex
 507 classes.

508 **Proof.** Suppose a vertex class P_i has $L_i(D)$ as the border which is part of the soup D ;
 509 $V(L_i(D))$ belong to P_i . Let S_D be the set of singletons participating in soup D . Let INS be
 510 the set of indices of non-singleton vertex classes that meet D (non-trivial vertex classes that
 511 participate in D , or that give the main border of D), and let $l_i = |V(L_i(D))|$ when $i \in INS$.
 512 Let b_i be the number of blocks of such an $L_i(D)$.

513 As $l_i \geq 2$, the edges of $L_i(D)$ v-cover exactly $l_i + b_i - 1$ relevant facial triangles of the
 514 soup D , as the walk around $L_i(D)$ has length exactly $l_i + b_i - 1$. A relevant triangle of soup
 515 D that is covered by a vertex class is v-covered exactly once during these walks around all
 516 the $L_i(D)$.

517 The total number of relevant facial triangles in the soup D is $2(S_D + \sum_{i \in INS} l_i) - 4 -$
 518 $\sum_{i \in INS} (l_i - b_i - 1)$, which is obtained as described in this paragraph. Construct a plane
 519 graph H' as follows. Start with H' being the soup D (which is a plane graph). Then all the
 520 relevant facial triangles of D are faces of H' . Take a B_i (given by the non-trivial vertex class
 521 P_i) that participates in the soup. Keep only $L_i(D)$ from B_i and triangulate every inner face
 522 of $L_i(D)$. This way, for B_i , we get exactly $l_i - b_i - 1$ triangular faces of H' that are not the
 523 faces of relevant facial triangles of D . Assume now that D has a main border and is given
 524 by vertices of B_i ; let F be the face of B_i used in the definition of soup D . Triangulate all
 525 the inner faces of $L_i(D)$ except for F , and triangulate the outer face of $L_i(D)$. Again, for
 526 B_i , we get exactly $l_i - b_i - 1$ triangular faces of H' that are not the faces of relevant facial
 527 triangles of D . Now H' is a triangulated graph with $2(S_D + \sum_{i \in INS} l_i)$ vertices, and has
 528 exactly $2(S_D + \sum_{i \in INS} l_i) - 4$ triangular faces. These are all faces of relevant facial triangles
 529 of D except for the $\sum_{i \in INS} (l_i - b_i - 1)$ faces that we described above.

530 Thus the number of relevant facial triangles of D that are not covered by vertex classes
 531 is exactly:

$$532 \quad 2(S_D + \sum_{i \in INS} l_i) - 4 - \sum_{i \in INS} (l_i - b_i - 1) - \sum_{i \in INS} (l_i + b_i - 1) = 2(S_D + |INS|) - 4 = 2g - 4.$$

533 This concludes the proof of the claim. ■

534 Note that when $g = 2$, this number is 0 (which we have seen before, when we looked at
 535 moats whose outside border is included in one vertex class). When $g > 2$, there are relevant
 536 facial triangles in D that are not covered by vertex classes, and thus must be covered by an
 537 edge color Q_j (just one color, from our second condition). Condition 4 of $(\mathcal{P}, \mathcal{Q})$ implies that
 538 edge color Q_j only covers relevant facial triangles of D , and in fact we can assume edge color
 539 Q_j only contains edges of D . Thus Q_j only covers facial triangles of D ; as the facial triangles
 540 of D that are not relevant (if any) are covered by a vertex class, we conclude that Q_j covers
 541 a set of facial triangles that is exactly the set of relevant facial triangles of D not covered by
 542 a vertex class. Recall that u_j is the number of vertex classes incident to edge color j . We
 543 have that $u_j = g$, based on earlier arguments when walking around moats with the space of
 544 moats of a soup being "connected". One can easily check that $2g - 4 = 2u_j - 4 \leq 4\lfloor \frac{u_j - 1}{2} \rfloor$,
 545 and therefore

$$546 \quad coverage(j) = 2g - 4 \leq 4\lfloor \frac{u_j - 1}{2} \rfloor, \tag{9}$$

547 where $coverage(j)$ is the number of facial triangles covered by edge color Q_j . Using Condition
 548 1 above, every facial triangle covered by an edge color is a relevant triangle in some soup and
 549 thus, using Condition 4, the equation above holds for all edge colors.

550 We have $2n - 4$ facial triangles that need to be covered by double-partition $(\mathcal{P}, \mathcal{Q})$ in
 551 \tilde{H} . Define $\lambda_i = 3p_i - 6 - E(B_i)$, the number of edges missing from B_i to be triangulated
 552 (we used here that $p_i = |V(B_i)| \geq 3$, from Condition 5). Each edge of B_i can v-cover at
 553 most two facial triangles of \tilde{H} . But there is an exception: if three edges of B_i form a facial
 554 triangle of \tilde{H} , then we must subtract 2 (as this facial triangle is covered three times when we
 555 computed above). Let \tilde{f}_i^3 be the number of faces of B_i that are faces of \tilde{H} . We obtain that
 556 the vertex class $V(B_i)$ can cover at most $2(3p_i - 6 - \lambda_i - \tilde{f}_i^3)$ facial triangles. Based on this
 557 discussion we have

$$2n - 4 \leq 2 \sum_{i=1}^h (3p_i - 6 - \lambda_i - \bar{f}_i^3) + \sum_{j=1}^q \text{coverage}(j), \quad (10)$$

where as before h is the number of non-trivial vertex classes of \mathcal{P} and q is the number of edge colors of \mathcal{Q} .

Let $p = \sum_{i=1}^h p_i$, $\bar{f} = \sum_{i=1}^h \bar{f}_i^3$, and $\lambda = \sum_{i=1}^h \lambda_i$. Let c' be the number of triangular faces of all B_i that contain exactly one singleton (of the double-partition) and no other vertex of \tilde{H} . This singleton is a cubic vertex of \tilde{H} . Let d be the number of triangular faces of all B_i that contain exactly two singletons, and no other vertex of \tilde{H} . Let s be the number of singletons of \mathcal{P} that are embedded in a triangular face of some B_i , where all the vertices of \tilde{H} contained in this face are singletons, and there are at least three of them. Let s' be the number of the other singletons of \mathcal{P} , not as above. Then $n = p + c' + 2d + s + s'$. From Equation (10) we deduce:

$$2(p + c' + 2d + s + s') - 4 \leq 6p - 12h - 2\lambda - 2\bar{f} + \sum_{j=1}^q \text{coverage}(j),$$

from which we deduce:

$$2s + 2c' + 4d + 2s' + 8h + 2\lambda + 2\bar{f} - 4 \leq 4p - 4h + \sum_{j=1}^q \text{coverage}(j).$$

Recall that k is the number of parts (vertex classes) of \mathcal{P} , h is the number of non-trivial vertex classes of \mathcal{P} , and p is the total number of vertices in non-trivial vertex classes. The contribution of \mathcal{P} to $\Phi(\mathcal{P}, \mathcal{Q})$ is $n - k = \sum_{i=1}^h (p_i - 1) = p - h$. Thus, using Equation (9),

$$\frac{1}{2}s + \frac{1}{2}c' + d + \frac{1}{2}s' + 2h + \frac{1}{2}\lambda + \frac{1}{2}\bar{f} - 1 \leq \Phi(\mathcal{P}, \mathcal{Q}). \quad (11)$$

Recall that each B_i is a connected plane graph with $|V(B_i)| = p_i \geq 3$. If it were triangulated, B_i would have exactly $2p_i - 4$ triangular faces. B_i is missing λ_i edges, and each of these can destroy at most two triangular faces. So we have at least $2p_i - 2\lambda_i - 5$ inner triangular faces of B_i . If F , one of these inner triangular faces of B_i , contains some B_j , then we call F a *green* face. For a green face F of B_i , there exists a $j \neq i$, with B_j contained in F and such that there is no $k \notin \{i, j\}$ with B_k contained in F and B_j in an inner face of B_k . We say that B_j *compels* F to become a green face and we note that B_j can only compel one face to become green. Thus there are at most h green faces. Let r_i be the number of non-green inner triangular faces of B_i that are not empty of points of \tilde{H} and let $r = \sum_{i=1}^h r_i$. Based on the discussion above, we have:

$$r \geq 2p - 2\lambda - 5h - \bar{f} - h = 2p - 6h - 2\lambda - \bar{f}. \quad (12)$$

From the definition of s ,

$$s \geq 3(r - c' - d)$$

as triangular faces of some B_i that are non-empty and non-green contain either one singleton (there are at most c' such faces), or two singletons (there are at most d such faces) or contain three or more singletons. From this and Equation (12) we obtain:

$$s + 3c' + 3d \geq 3(2p - 6h - 2\lambda - \bar{f})$$

593 and therefore:

$$594 \quad 7s + 7c' + 14d + 28h + 7\lambda + 7\bar{f} \geq 6p + 6s + 6c' + 12d - 2(c' + d) + 10h,$$

595 which implies, as $n = p + s + c' + 2d + s'$, that

$$596 \quad \frac{1}{2}s + \frac{1}{2}c' + d + \frac{1}{2}s' + 2h + \frac{1}{2}\lambda + \frac{1}{2}\bar{f} - 1 \geq \frac{3}{7}n - \frac{1}{7}(c' + d) + \frac{5}{7}h - 1 \geq \frac{3}{7}n - \frac{1}{7}c - 1,$$

597 where for the last inequality we use the fact that $c \geq c' + d$, which follows from the fact
 598 that if two vertices are embedded in a triangular face, and together with the triangle form
 599 a triangulated planar graph, then one of these two vertices is cubic. This combined with
 600 Equation (11) implies Equation (3), finishing the proof of Theorem 5. ■

601 **We continue the analysis of the approximation ratio of Algorithm MTLK4.** As
 602 before, G denotes the input graph and H an optimum solution (a maximum planar subgraph
 603 of G). Let \tilde{H} be a triangulated plane supergraph of H , and θ be $|E(\tilde{H})| - |E(H)|$. As above,
 604 the value of the optimum solution is $|E(H)| = 3n - 6 - \theta$. Below, c counts the number of
 605 cubic vertices in \tilde{H} .

606 From Theorem 5 and Proposition 2 we immediately obtain

$$607 \quad \beta(G) \geq \beta(H) \geq \beta(\tilde{H}) - \theta \geq \frac{3}{7}n - \frac{1}{7}c - \theta - 1 \quad (13)$$

608 as one edge of $E(\tilde{H}) \setminus E(H)$ can be part of only one triangle of the maximum triangular
 609 cactus of \tilde{H} .

610 Let A be the kt-structure produced by MTLK4. Say that there is a *strong bond* between
 611 two vertices if there is a path between them in A with all edges in K_4 's of A . Call a cubic
 612 vertex v of \tilde{H} *blocked* if $K_4(v)$, the K_4 formed by v and its three neighbors in \tilde{H} , is not added
 613 to the kt-structure. A cubic vertex v is blocked because of one of the following:

- 614 ■ one of the edges of $K_4(v)$ is not in G (also not in H). We call v *absent*.
- 615 ■ all the edges of $K_4(v)$ are in G (and in H - since H is a maximum planar subgraph of G)
 616 and at least two of the four vertices of $K_4(v)$ are connected by a strong bond. We call v
 617 *neutralized*.
- 618 ■ all the edges of $K_4(v)$ are in G (and in H) and there are no strong bonds between any
 619 of the vertices of $K_4(v)$, and all four of the vertices of $K_4(v)$ are in the same connected
 620 component of A . We call v *subdued*.

621 Indeed, if all the edges of $K_4(v)$ are in G (and in H) and there is no strong bond between
 622 any two vertices of $K_4(v)$ and only three of its vertices are in the same component of A ,
 623 then we could remove at most two triangles from this component of A to disconnect these
 624 three vertices, and add $K_4(v)$ while maintaining a kt-structure. Also, assuming there is no
 625 strong bond between any two vertices of $K_4(v)$: if two of the vertices of $K_4(v)$ are in one
 626 component of A and the other two in another component of A , then we can remove one
 627 triangle from each of these two components and add $K_4(v)$ while maintaining a kt-structure,
 628 and if the vertices of $K_4(v)$ are in three or four components of A , it is easy to remove just
 629 one triangle from A and add $K_4(v)$ while maintaining a kt-structure.

630 We use c_a to denote the number of absent cubics, c_s to denote the number of subdued
 631 cubics, and let c_n be the number of neutralized cubics. Let $A'_1, \dots, A'_{q'}$ be the non-trivial
 632 sub-kt-structures obtained from A by removing all the triangles that are not part of K_4 's. If
 633 we have j'_i K_4 's in A'_i , then A'_i has $3j'_i + 1$ vertices, each two of them connected by a strong
 634 bond. All the strong bonds are obtained this way. Let γ be the number of K_4 's in A . Then
 635 $\gamma = \sum_{i=1}^{q'} j'_i$.

636 Let B'_i be $\tilde{H}[V(A'_i)]$. Then B'_i has at most $3(1 + 3j'_i) - 6 = 9j'_i - 3$ edges. For a cubic v
 637 to be neutralized, one of the four edges of $K_4(v)$ must be an edge of some B'_i . Recall than
 638 $n > 4$ and that \tilde{H} is a triangulated plane graph. Then cubic vertices cannot be adjacent
 639 in \tilde{H} and one can easily check that one edge e of \tilde{H} can participate in at most two $K_4(u)$.
 640 Precisely, if one of the endpoints of e is a cubic, then this endpoint is the only possible u
 641 above, and if not, then the only possible u above are the two vertices that each forms a facial
 642 triangle with e .

643 Thus the total number of neutralized cubics is at most

$$644 \quad c_n \leq 2 \sum_{i=1}^{q'} (9j'_i - 3) \leq 18\gamma. \quad (14)$$

645 Also by the reasoning above,

$$646 \quad c_a \leq 2\theta. \quad (15)$$

647 Let α be the number of triangles in A and recall that γ is the number of K_4 's in A .
 648 Let A have non-trivial components A_1, \dots, A_q , each with α_i triangles and γ_i K_4 's. Let
 649 $B_i = \tilde{H}[V(A_i)]$. Thus $|V(B_i)| = |V(A_i)| = 1 + 2\alpha_i + 3\gamma_i$. Now we count how many subdued
 650 cubics $c_s(i)$ are in $V(A_i)$. Remove all these cubics from B_i and we get a planar graph D_i
 651 with $1 + 2\alpha_i + 3\gamma_i - c_s(i)$ vertices and where each subdued cubic vertex of A_i is the only
 652 vertex of \tilde{H} embedded in a triangular face of D_i (recall that $n > 4$ and cubic vertices cannot
 653 be adjacent in \tilde{H}). We know that D_i can have at most $2(1 + 2\alpha_i + 3\gamma_i - c_s(i)) - 4$ triangular
 654 faces, and thus:

$$655 \quad c_s(i) \leq 2(1 + 2\alpha_i + 3\gamma_i - c_s(i)) - 4$$

656 from which we deduce:

$$657 \quad c_s \leq \frac{4}{3}\alpha + 2\gamma - \frac{2}{3}q$$

658 (recall that here q is the number of non-trivial components of A). As $\alpha \leq \beta(G)$ (recall that
 659 $\beta(G)$ is the number of triangles in a maximum triangular cactus of the graph G), adding the
 660 equation above to Equations (14) and (15) we obtain:

$$661 \quad c \leq 20\gamma + \frac{4}{3}\beta(G) + 2\theta,$$

662 which we rewrite as

$$663 \quad \gamma \geq -\frac{1}{15}\beta(G) - \frac{1}{10}\theta + \frac{1}{20}c. \quad (16)$$

664 Now we have all the ingredients to obtain our $((4/9) + \epsilon)$ -approximation. As before, G
 665 denotes the input graph and H an optimum solution (a maximum planar subgraph of G).
 666 Let \tilde{H} be a triangulated plane supergraph of H , and θ be $|E(\tilde{H})| - |E(H)|$. As above, the
 667 value of the optimum solution is $|E(H)| = 3n - 6 - \theta$. From Inequality (3) for H , we obtain:

$$668 \quad \beta(G) \geq \beta(H) \geq \frac{1}{3}(n - 2 - \theta).$$

669 Multiply the inequality above by 141/166, Inequality (13) by 21/166, and Inequality (16)
 670 by 60/166 (we solved by hand a small linear program to obtain these numbers) and add
 671 them up to obtain:

$$\beta(G) + \gamma \geq \beta(G) + \frac{60}{166}\gamma \geq \frac{28}{83}n - \frac{37}{83}\theta - 1.$$

As every K_4 introduced by the algorithm gains at least one more edge compared to the one or two triangles it replaces (in other words, it increases the cyclomatic number by at least one), our output has at least $n - 1 + \beta(G) + \gamma$ edges. Based on the inequality above, one can check that

$$n - 1 + \beta(G) + \gamma \geq \frac{111}{83}n - \frac{37}{83}\theta - 2 \geq \frac{37}{83}(3n - \theta - 6).$$

In conclusion, we have:

► **Theorem 7.** *Algorithm MTLK₄ is a (37/83)-approximation for MPS.*

The improvement $\epsilon = 1/747$.

4 Local Optimization without Max Triangular Cactus

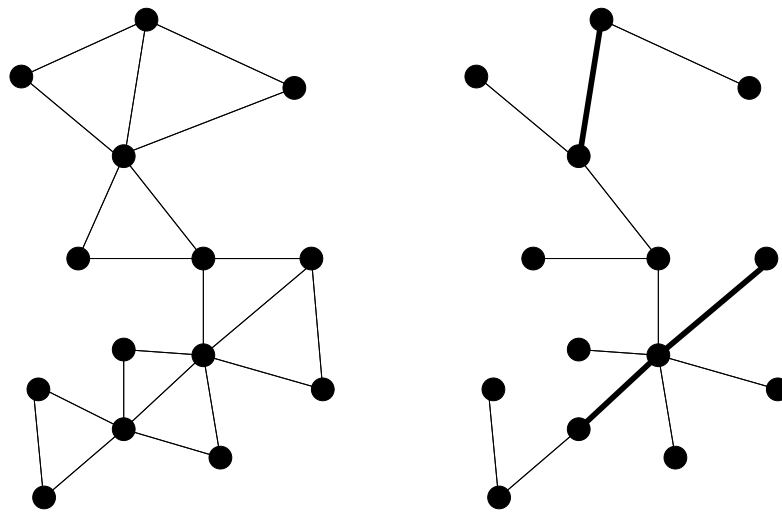
Recall that a diamond subgraph is a graph that is isomorphic to the graph resulting from deleting any single edge from a K_4 . We call the two vertices of degree three in a diamond as the bases of the diamond, and the two vertices of degree two as the tips of the diamond. We call the edge between the two bases of a diamond the base-edge of the diamond. A diamond of a plane graph is a *facial diamond* if the two triangles of the diamond are facial triangles.

In this section, we present **LDT**, a local optimization algorithm (inspired by the one of [6]) using only diamonds and triangles that is a (5/12)-approximation algorithm for MPS on general graphs. There is a tight example for this approximation ratio. The input is a graph G , which we assume to be connected as one can run any approximation algorithm on separate connected components if needed.

4.0.0.1 Algorithm LDT:

We maintain a spanning subgraph A (thus $V(A) = V(G)$) that is a dt-structure in G , starting with $E(A) = \emptyset$. The algorithm has two phases.

Phase I: The goal of this phase is to increase the cyclomatic number of A . For each connected component A' of A , the algorithm keeps a weighted tree $T_{A'}$ whose vertex set is $V(A')$ and edge set is as follows (see Figure 10 for an illustration). For every diamond of A , the edge connecting the bases is included in $T_{A'}$ with weight 2. For each of the two tips of every diamond, include in $T_{A'}$ an edge between this tip and one of the bases, with weight 1. For every triangle of A' , include in $T_{A'}$ two of its edges, each with weight 1. One can easily check that $T_{A'}$ is a spanning tree of A' . Let $F(A)$ be the spanning forest on $V(G)$ obtained by taking all the edges of $E(T_{A'})$ for all the components A' of A .

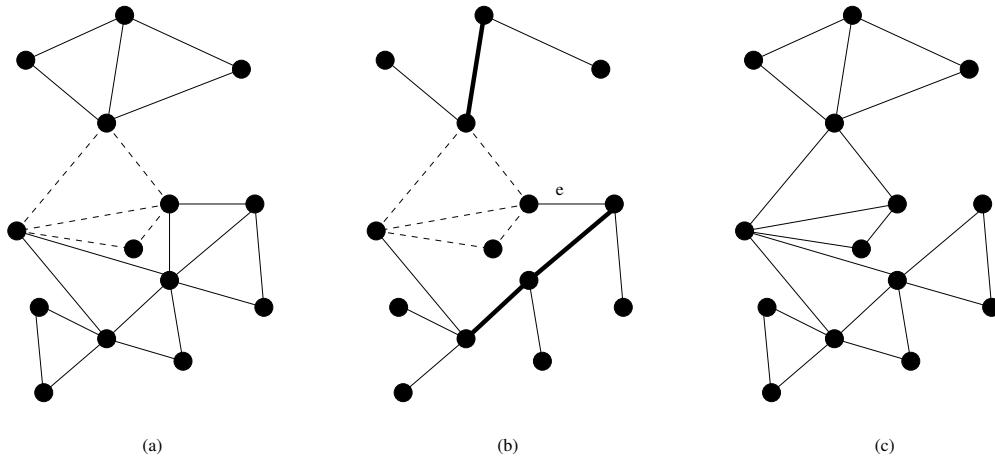


■ **Figure 10** On the right, the tree $T_{A'}$ obtained from a connected component A' (depicted on the left) of A . Edges of weight 2 are thick

703 One local optimization step is obtained as follows: if there exist a triangle of G with
 704 its three vertices in three different components of A , then add this triangle to A , and
 705 resume. If no such triangle exists, go through all the diamonds D of G . Go through all
 706 the edges $e \in E(F(A))$ of weight 1. Let $F_e(A)$ be the spanning forest of G whose edge
 707 set is $E(F(A)) \setminus \{e\}$. If the four vertices of D are in four components of $F_e(A)$, and e
 708 was in $E(F(A))$ as an edge of a triangle, then remove from A this triangle and add D . If
 709 the four vertices of D are in four components of $F_e(A)$, and e was in $E(F(A))$ as an edge
 710 that connects a tip of a diamond D' to one of the bases of D' , then remove from A the
 711 two edges connecting this tip from the bases (leaving a triangle from the diamond D')
 712 and add D .

Phase II: As long as possible, greedily add edges connecting various components in graph $(V(A), E(A))$
 714 to get the output L (L is connected since the input G is connected).

715 See Figure 11 for an example of a local optimization step. One can easily check that
 716 applying the local optimization step of Phase I keeps A a dt-structure and its cyclomatic
 717 number indeed increases.



■ **Figure 11** (a) shows in solid line segments the current dt-structure A . A diamond D , represented by the dashed line segments, is considered. (b) A forest $F(A)$ is represented by thick solid line segments having weight 2 and thin solid line segments having weight 1. We can see that by removing from $F(A)$ the weight-1 edge e , the four vertices of the diamond D are in four different components. (c) The resulting dt-structure after the local optimization step.

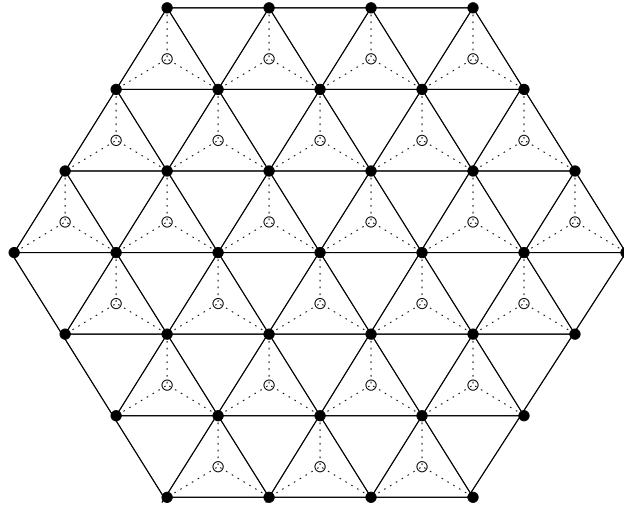
718 **Running time** We discuss the running time of one local improvement, or finding out
 719 that no such improvement exists. There are $O(n)$ edges in the current dt-structure A . Using
 720 Depth First Search, computing the connected components of the current dt-structure can be
 721 done in $O(n)$. There are $O(n^3)$ triangles in the input graph. Using the information given
 722 by the connected components of the current dt-structure, it takes constant time to check
 723 whether a triangle can be used for improving the dt-structure (this involves finding, for each
 724 vertex v of the triangle, the representative of the connected component containing v , and
 725 then checking if we have three distinct representatives). For the local optimization using
 726 diamonds, we use a more elaborate method to save a factor of n in the running time.

727 Let $\hat{F}(A)$ be the spanning forest on $V(G)$ obtained by taking all the edges of $E(T_{A'})$
 728 that have weight 2, for all the components A' of A . We construct $\hat{F}(A)$ and, using Depth
 729 First Search, compute its connected components in time $O(n)$. Then we go through all the
 730 $O(n^4)$ diamonds and for each such diamond D we check if its four vertices belong to at
 731 least three connected components of A . If no, D cannot be used. If yes, we check if the
 732 two nodes that are in the same connected component of A are also in the same connected
 733 component of $\hat{F}(A)$; if yes, then D cannot be used. If no, in time $O(n)$ we can find one edge
 734 $e \in F(A) \setminus \hat{F}(A)$ such that the four vertices of D are in four different components of $F_e(A)$.
 735 In time $O(n^4)$ we can easily update A to include D .

736 There are $O(n)$ local improvement steps, for a total running time of $O(n^5)$.

737 **Approximation Ratio Analysis** First we show that the approximation ratio does not
 738 exceed $5/12$ by more than an $o(1)$ term. Consider a large triangular grid H as in Figure 12,
 739 which occupies a regular hexagon, and such that H has an odd number of vertices, $2p + 1$,
 740 with a large p . Let S be some triangular cactus, with p triangles, and with $V(S) = V(H)$.
 741 We make S edge-disjoint from H , and also we avoid having the endpoints of an edge of S
 742 at distance less than 2 in H . One can easily check that H has $4p - o(p)$ faces. In “every
 743 second” face of H add a “new” point as in the figure, so that points are not added in two
 744 faces of H that share an edge in H . Connect each of these new points to the three vertices
 745 of H lying on the border of the face of H where the new point is added. The input graph G
 746 consists of the union of H and S and these new points with their incident new edges. Thus

747 G has $4p - o(p)$ vertices. The union of H and the new points induces an almost triangulated
 748 planar graph with $12p - o(p)$ edges. The triangular cactus S can be the solution produced
 749 by the Phase I of the algorithm, as we show in the next paragraph. Then our output has no
 750 diamonds and p triangles, for a total of at most $5p$ edges (the output has cyclomatic number
 751 of p and less than $4p$ vertices). By choosing p as large as we wish, we get a ratio as close to
 752 $5/12$ as we want.



■ **Figure 12** The planar graph H is given by filled circles representing the vertices and solid lines representing the edges. The new vertices are represented by empty circles, and the edges adjacent to these new vertices are represented by dashed lines.

753 It is easy to check that no triangle can be added to S . Now we check that no diamond can
 754 be swapped for a triangle in S according to Phase I of the algorithm. From our construction,
 755 any diamond of G has at least three vertices in $V(S)$, and for any edge e from $E(F(E(S)))$,
 756 the graph $F_e(E(S))$ will have one component with at least two of these three vertices.

757 We continue with the proof that the approximation ratio of LDT is at least $5/12$. Recall
 758 that G , the input graph, is connected and let OPT be an optimal MPS solution of G . Define
 759 $n := |V(G)| = |V(OPT)|$. We fix a planar embedding of OPT which will be used through
 760 out the section. Add to OPT a set Θ of edges to obtain a triangulated simple plane graph
 761 H . Let $\theta := |\Theta|$. A triangulated plane graph with n vertices has $3n - 6$ edges, if $n \geq 3$. So
 762 $\theta = (3n - 6) - |E(OPT)|$; θ does not depend on the embedding of OPT or H .

763 Let A be the dt-structure at the end of Phase I of the LDT algorithm. Let A have c
 764 non-trivial connected components A_1, A_2, \dots, A_c . Let t_i, d_i be the number of triangles and
 765 diamonds in A_i respectively. This implies that the number of vertices n_i in the component
 766 A_i is exactly $3d_i + 2t_i + 1$ and the number of edges in A_i is exactly $5d_i + 3t_i$.

767 Let $d := \sum_{i=1}^c d_i$ and $t := \sum_{i=1}^c t_i$. We can also see that the output L has $(n - 1) + 2d + t$
 768 edges, as every diamond adds two edges and every triangle adds one edge to a spanning tree
 769 (recall that the input graph G is connected and thus has a spanning tree).

770 First, we notice that if $c = 0$ (there are no triangles in G), then OPT has no triangle
 771 and it is a simple exercise that OPT has at most $2n - 2$ edges (this follows from Euler's
 772 formula and the fact that all the faces of an embedding of OPT have at least four edges
 773 on their boundary). As Phase II produces a graph with at least $n - 1$ edges, we have a
 774 $(1/2)$ -approximation. Thus, from now on, we assume $c \geq 1$.

775 Second, we notice that, unless n is large compared to d and t , we get the desired
 776 approximation ratio. Precisely,

$$777 \quad \frac{(n-1) + 2d + t}{3n - 6 - \theta} \geq \frac{(n-1) + 2d + t}{3n - 6} \geq \frac{5}{12}$$

778 if $n \leq 8d + 4t + 6$. So from now on, we assume that:

$$779 \quad n > 8d + 4t + 6. \tag{17}$$

780 Let $B_i := H[V(A_i)]$ be the subgraph of H induced by the vertices of A_i . Then we have
 781 $n_i = |V(B_i)|$. Let $m_i := |E(B_i)|$.

782 In T_{A_i} , defined in the description of Phase I of the LDT algorithm (also illustrated in
 783 Figure 10), remove the edges of weight 1 and we are left with several connected non-trivial
 784 components $J_i^1, J_i^2, \dots, J_i^{k_i}$, where $k_i > 0$ if $d_i > 0$ (if $d_i = 0$ there are no weight-2 edges in
 785 T_{A_i} and there are no non-trivial components above). The graphs $H[V(J_i^j)]$ are all planar
 786 and each can have at most $3|V(J_i^j)| - 5 = 3(|V(J_i^j)| - 1) - 2$ edges. Note that J_i^j uses
 787 $(|V(J_i^j)| - 1)$ weight-2 edges in T_{A_i} . We have d_i weight-2 edges in T_{A_i} . From this we obtain
 788 that the total number α_i of all edges of all the k_i graphs $H[V(J_i^j)]$ cannot exceed $3d_i - 2$:

$$789 \quad \alpha_i \leq 3d_i - 2 \tag{18}$$

790 No border of a triangular face f of H can be added to A in **Phase I**, and based on this
 791 we classify all the triangular faces of H into one of the following three categories:

792 **Category 1:** at least one edge bordering f is in Θ (and the triangle given by the border of
 793 f does not exist in OPT ; recall that Θ is the set of edges we have added to OPT to obtain
 794 the triangulated plane graph H).

795 **Category 2:** no edge bordering f is in Θ and exactly two vertices on the border of f are in
 796 the same $V(B_i)$.

797 **Category 3:** no edge bordering f is in Θ and all three vertices on the border of f are in the
 798 same $V(B_i)$.

799 There are $2n - 4$ triangular faces of H and at most 2θ can fall in the first category above,
 800 as one edge of Θ only borders two triangular faces of H . Therefore at least $2n - 4 - 2\theta$
 801 triangular faces fall in either the second or the third category.

802 If an edge of B_i borders two triangular faces in the second category above, we call it a
 803 *strong* edge of B_i , and let S_i be the set of strong edges of B_i ; also let $s_i = |S_i|$. The other
 804 edges of B_i are called *weak* edges. A weak edge can border at most one triangular face in
 805 the second category, and can border triangular faces in the third category. Think of this
 806 weak edge as contributing 1 to the Category 2 triangular faces and $1/3$ to the Category 3
 807 triangular faces. With these reasonings, we obtain:

$$808 \quad \sum_{i=1}^c (2s_i + (4/3)(m_i - s_i)) \geq 2n - 4 - 2\theta,$$

809 which we rewrite as

$$810 \quad \sum_{i=1}^c ((2/3)s_i + (4/3)m_i) \geq 2n - 4 - 2\theta. \tag{19}$$

811 Define Γ_i to be the set of (strong) edges in S_i that are not in any of the k_i graphs $H[V(J_i^j)]$
 812 mentioned above, and let $\Gamma = \cup_i \Gamma_i$. (This set Γ will give us technical issue complicating
 813 the proof.) Let $\gamma_i := |\Gamma_i|$, and note that $s_i \leq \alpha_i + \gamma_i$. The graph B_i does not have to be

814 triangulated; let $\lambda_i := 3n_i - 6 - m_i$ (λ_i is the number of edges missing from B_i to make a
815 triangulated planar graph, noting that $n_i \geq 3$).

816 Then from $s_i \leq \alpha_i + \gamma_i$ and Inequality (19) we obtain

$$817 \quad \sum_{i=1}^c ((2/3)(\alpha_i + \gamma_i) + (4/3)(3n_i - 6 - \lambda_i)) \geq 2n - 4 - 2\theta,$$

818 which we rewrite as

$$819 \quad \sum_{i=1}^c \left(\frac{2}{3}\alpha_i + 4n_i - 8 \right) + \sum_{i=1}^c \left(\frac{2}{3}\gamma_i - \frac{4}{3}\lambda_i \right) \geq 2n - 4 - 2\theta. \quad (20)$$

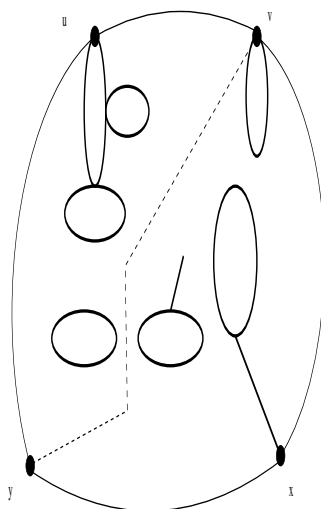
▷ Claim 8.

$$820 \quad \sum_{i=1}^c \gamma_i \leq 5c + 2 \sum_{i=1}^c \lambda_i. \quad (21)$$

821 We believe that a stronger inequality holds, maybe without a 2 in front of the second
822 summation; however this is enough for our purposes. We are unable to prove this without a
823 long charging argument.

824 **Proof.** We first add some notation. The graphs B_i are considered plane graphs here. We
825 add and embed a set of edges Λ_i to B_i to obtain a triangulated plane (simple) graph, and thus
826 we will have $|\Lambda_i| = \lambda_i$. We do this carefully as follows. Let B_i^j , $j = 1, 2, \dots, j_i$ be the connected
827 components of B_i , and let $b_i^j = |V(B_i^j)|$. Out of these connected components, let \bar{j}_i be the
828 number of the trivial components, with only one vertex each (also called *singletons*), and let
829 \hat{j}_i be the number of components with two vertices only; we call such a component a *doubleton*.
830 If $b_i^j > 2$, let $B_i^j(l)$, for $l = 1, 2, \dots, l_i^j$, be the blocks of B_i^j , and let $b_i^j(l) = |V(B_i^j(l))|$. Note
831 that $b_i^j(l) \geq 2$. Let \bar{l}_i^j be the number of trivial blocks of B_i^j , meaning with two vertices (these
832 trivial blocks are the *bridges* of the connected component B_i^j).

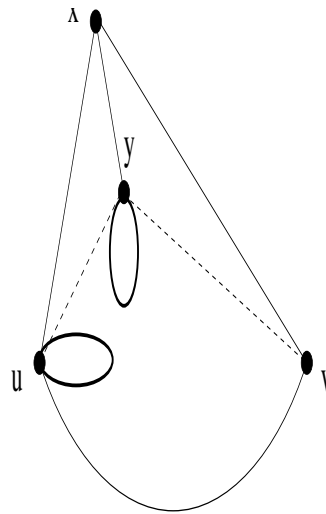
833 To construct Λ_i , we start by looking at non-trivial blocks $B_i^j(l)$, and add (and embed) a
834 set of “diagonal” edges Δ_i in each face of each $B_i^j(l)$ until $B_i^j(l)$ becomes triangulated. See
835 Figure 13 for an illustration. It is easy to check that this keeps the graph with vertex set
836 $V(B_i)$ and edge set $E(B_i) \cup \Delta_i$ simple and plane; moreover each of this graph’s non-trivial
837 blocks is a triangulated plane graph.



■ **Figure 13** An illustration of adding edges in Δ_i . Here we have the bounded face with corners u, v, x, y of some $B_i^j(l)$. Other blocks or components of B_i that are embedded in this face are depicted by thick ovals. We can add and embed the diagonal edge vy , depicted by the dashed poly-line, while maintaining a plane embedding.

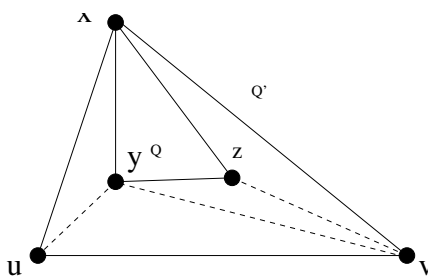
838 Next, as long as we have a trivial block (a bridge yx) sharing an endpoint x with a trivial
 839 block xz , we add the edge yz while maintaining planarity. This results in some triangulated
 840 blocks. Let Ω_i be the set of such edges added while doing this.

841 Next, if we have a trivial block (a bridge yx) sharing an endpoint x with a non-trivial
 842 block Q , and y is embedded in a face xuv of Q , we add the edges uy and vy resulting in a
 843 bigger planar block that contains y and the vertices of Q ; see Figure 14 for an illustration.
 844 This bigger block is triangulated. Let Π_i be the edges added in this phase. The resulting
 845 graph is still planar.

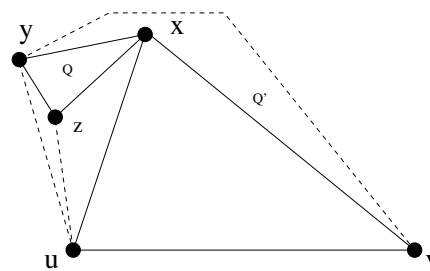


■ **Figure 14** An illustration of adding edges in Π_i to merge the bridge xy into the block Q that has the vertices x, u, v such that y is embedded in a triangular face of Q . Here the starting edges are thin continuous segments or arc segments, and the new edges added to Π_i are dashed segments. We can do this even if some other blocks contain x or y or u or v . Two such block are depicted as the thick ovals. While in this figure y is embedded in an inner face of Q , the same idea can be used when y is embedded in the outer face of Q .

846 Next, we consider two non-trivial blocks that share one vertex x (an articulation point).
 847 All blocks except doubletons are triangulated by now. One block Q with outer face triangle
 848 xyz is embedded in a face xuv of the other block Q' . We add three edges to make $Q \cup Q'$
 849 triangulated, as in Figure 15. We repeat this process, until all the blocks in the same
 850 component of B_i are merged together into one plane block; this is a triangulated plane graph
 851 except for doubletons. Let Υ_i be the set of such “reinforcing” edges added while doing this.
 852 (We could but do think of the edges of $\Omega_i \cup \Pi_i$ as “reinforcing” a connected component
 853 since their goal in this proof is to eliminate the bridges).



An illustration of adding edges in Υ_i to merge a block Q with outer face xyz into the block Q' , where y and z are embedded in an inner triangular face of Q' that has as corners the vertices x, u, v . Here the starting edges are thin continuous segments, and the new edges added to Υ_i are dashed segments.



An illustration of adding edges in Υ_i to merge a block Q with outer face xyz into the block Q' , where y and z are embedded in the outer triangular face of Q' that has as corners the vertices x, u, v . Here the starting edges are thin continuous segments, and the new edges added to Υ_i are dashed segments.

■ **Figure 15** Merging two non-trivial blocks

854 Thus, the graph with vertex set $V(B_i)$ and edge set $E(B_i) \cup \Delta_i \cup \Omega_i \cup \Pi_i \cup \Upsilon_i$ is planar;
 855 by now each of its connected components with at least three vertices is a triangulated plane
 856 graph. We have that the number of bridges of B_i that are not doubletons is at most

$$857 \quad 2|\Omega_i \cup \Pi_i| \tag{22}$$

858 as any such bridge disappears when we add $\Omega_i \cup \Pi_i$ and one edge of $\Omega_i \cup \Pi_i$ results in the
 859 disappearance of at most two such bridges. Precisely, an edge of Ω_i makes two bridges
 860 disappear (meaning that the edge that is a bridge does not form a bridge any more), two
 861 edges of Π_i make one bridge disappear.

862 Now we proceed to connect the graph G' , where $V(G') = V(B_i)$ and initially $E(G') =$
 863 $E(B_i) \cup \Delta_i \cup \Omega_i \cup \Pi_i \cup \Upsilon_i$. First let us assume that G' has a component Q with at least
 864 three vertices. This component will "absorb" other components as follows. All the other
 865 components are embedded in faces of Q . Pick a component Q' so that Q' is not embedded
 866 in an interior face of any other component of G' other than possibly Q . If Q' is a singleton x
 867 and is embedded in a faces uvw of Q , add three edges xu , xv , and xw to G' ; adjust Q to
 868 include vertex x and note that Q remains a triangulated plane graph. We are adding three
 869 edges per singleton. If Q' is a doubleton xy and is embedded in a (triangular) face of Q with
 870 corners u, v, w , add the five edges ux , vx , vy , wx , and wy to G' ; adjust Q to include vertices
 871 x and y , and note that Q remains a triangulated plane graph. We are adding five edges per
 872 doubleton.

873 If Q' has at least three vertices, it is a triangulated plane graph. We have three cases:
 874 Q' is embedded in an inner face of Q , or Q is embedded in an inner face of Q' , or each is
 875 embedded in the outer face of the other. The first two cases are symmetric and we only
 876 describe the first one below. Let x, y, z (clockwise order) be corners of the outer face of Q' .
 877 Here Q' is embedded in an inner face F' of Q ; let u, v, w (clockwise order) be the corners
 878 of F' . Add to G' the six edges: ux , uy , vy , vz , wz , and wx . See the left side Figure 16 for
 879 an illustration. Adjust Q to included Q' and note that it is triangulated plane graph. In
 880 the third case, Q' is embedded in the outer face F' of Q . let u, v, w (clockwise order) be the
 881 corners of F' . Add to G' the six edges: ux , uy , wy , wz , vz , and vx . See the right side of
 882 Figure 16 for an illustration. Adjust Q to included Q' and note that it is triangulated plane
 883 graph.

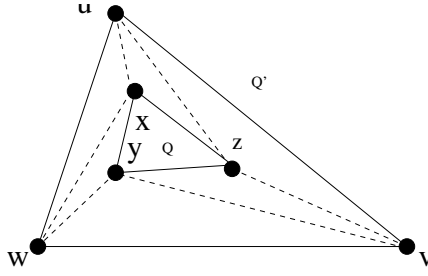
884 Keep doing this until G' is connected and triangulated; let Ψ_i be the set of edges added
 885 in this stage. Recall that j_i is the number of connected components of B_i , \bar{j}_i is the number of
 886 singletons and \hat{j}_i is the number of doubletons respectively. There are $(j_i - \bar{j}_i - \hat{j}_i)$ connected
 887 components of B_i that are not singletons nor doubletons. Thus:

$$888 \quad |\Psi_i| = 3\bar{j}_i + 5\hat{j}_i + 6(j_i - \bar{j}_i - \hat{j}_i - 1) \tag{23}$$

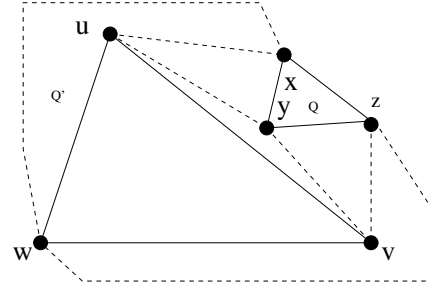
889 Second, assume that G' does not have components with at least three vertices. Then G'
 890 has $\bar{j}_i + 2\hat{j}_i$ vertices and \hat{j}_i edges. Note that $|V(G')| = |V(B_i)| \geq 3$. A triangulated graph
 891 with this many vertices would have $3(\bar{j}_i + 2\hat{j}_i) - 6$ edges and therefore a set Ψ_i with exactly
 892 $3\bar{j}_i + 5\hat{j}_i - 6$ edges can be added to G' to make it a plane triangulated simple graph. Note
 893 that Equation (23) still holds.

894 Finally $\Lambda_i = \Psi_i \cup \Omega_i \cup \Pi_i \cup \Upsilon_i \cup \Delta_i$. Recall that $\lambda_i = |\Lambda_i|$.

895 Our credit scheme starts with credits equal to the RHS of Inequality (21). These credits
 896 are given by a procedure we describe later to each components of every B_i , bridges of
 897 every B_i , and edges of $\Delta_i \cup \Upsilon_i$ ("diagonals" and "reinforcing"). These components, bridges,
 898 diagonals, and reinforcing edges pay, as described later, for all the edges Γ so that every edge
 899 of Γ receives one credit, and nobody uses more credit than it was allocated.



An illustration of adding edges in Ψ_i to merge a connected component Q' with outer face xyz with a connected component Q , where Q' is embedded in an inner triangular face of Q that has as corners the vertices u, v, w . Here the starting edges are thin continuous segments, and the new edges added to Ψ_i are dashed segments.



An illustration of adding edges in Ψ_i to merge a connected component Q with outer face uvw with a connected component Q' with outer face xyz , when Q is embedded in the outer triangular face of Q' and vice-versa. Here the starting edges are thin continuous segments, and the new edges added to Ψ_i are dashed segments.

■ **Figure 16** Merging two components of G'

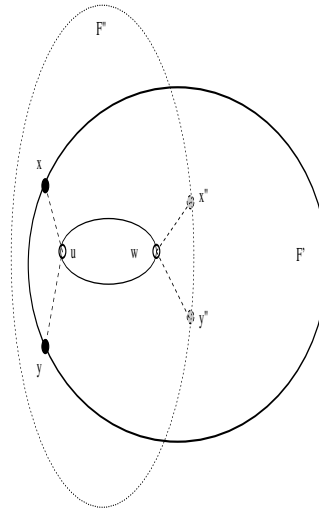
900 Precisely, we give $5 + 2\lambda_i$ credits to B_i , further allocated as follows. Every edge of Λ_i has
 901 2 credits. We keep 2 credits to every edge of Δ_i . We give one credit on every bridge of B_i
 902 that is not a doubleton; these credits come from $\Omega_i \cup \Pi_i$.

903 We give 3 credits on every connected component of B_i , and another 1 credit on every
 904 doubleton of B_i . These credits come from the 5 allocated to B_i , and from the edges of
 905 Ψ_i . To check that we have enough credits, we look at how Ψ_i is constructed. If B_i has
 906 one component with at least three vertices, then we give this component 3 credits from
 907 the 5 we have. Whenever we add another component of B_i with at least three vertices,
 908 we give this component 3 credits, from the 6 edges we are putting in Ψ_i . Whenever we
 909 add another component of B_i with 2 vertices (a doubleton), we give this component 4
 910 credits, from the 5 edges we are putting in Ψ_i . Whenever we add another component of
 911 B_i with 1 vertex (a singleton), we give this component 3 credits, from the 3 edges we are
 912 putting in Ψ_i . If B_i only has singletons and doubletons, we would need $3\bar{j}_i + 4\hat{j}_i$ credits,
 913 and we have two credits for every edge of Ψ_i , plus another 5 credits. In total, we have
 914 $5 + 2(3\bar{j}_i + 5\hat{j}_i - 6) = 3\bar{j}_i + 4\hat{j}_i + (3\bar{j}_i + 6\hat{j}_i - 7)$ credits, and this is enough since $3\bar{j}_i + 6\hat{j}_i \geq 9$
 915 (recall that here $\bar{j}_i + 2\hat{j}_i = n_i \geq 3$).

916 We continue with the proof of Inequality (21). Consider an edge $xy \in \Gamma_i$ (for some i),
 917 and let us look at the facial diamond D of H which has xy as a base. We name u and v the
 918 tips of D . Note that u cannot be in $V(B_i)$ since no facial triangle adjacent to xy has all
 919 three vertices in $V(B_i)$, since xy is a strong edge. Also, all the edges of this diamond are in
 920 OPT and therefore in the input graph G ; this follows from the fact that none of the edges
 921 of D are in Θ since, again, xy is strong. Same reasoning applies to show $v \notin V(B_i)$. And
 922 we must have the case that u and v are in the same $V(B_{i'})$, since otherwise the Phase I of
 923 the LDT algorithm will not stop yet, as argued next. Since $xy \in \Gamma_i$, x and y are not in the
 924 same $V(J_i^j)$, for some j . This means that there exists an edge e of T_{A_i} of weight 1 that can
 925 disconnect x from y in T_{A_i} . If u and v were not in the same $V(B_{i'})$, then u, v, x, y , the four
 926 vertices of D , would be in four components of $F_e(A)$ and another step of Phase I would be
 927 executed.

928 If the edge xy is a bridge of B_i , then we use one credit given to that bridge in the credits
 929 scheme to pay the edge; if this bridge is a doubleton, it still has three credits left. By now,
 930 the edges of Γ that are bridges in some B_i are all paid and every connected component of
 931 every B_i has at least three credits left. Also, every edge of each Δ_i has two credits left.

932 Assume now that xy is not a bridge of B_i and let F' be an interior face of B_i having xy
 933 as one of the edges bordering F' . We have that one of $\{u, v\}$ is embedded in F' and the
 934 other is embedded outside F' , as xyv and xyu are the two facial triangles of H adjacent to
 935 edge xy . Let us assume that u is embedded in F' ; then the whole component of $B_{i'}$ that
 936 contains u is embedded in F' . Moreover, there cannot be another inner face F'' of some $B_{i''}$
 937 such that the component of $B_{i''}$ that contains u is embedded in F'' and some vertex w of
 938 this component has two neighbors x'' and y'' in $B_{i''}$ such that there exists a triangular
 939 face of H with corners w, x'', y'' (see Figure 17). Traversing the boundary of the face F' we
 940 meet a total of f' edges once and b' edges twice (these are bridge edges of B_i). Note that
 941 these bridge edges, if they are in Γ_i , they are paid one credit each. To triangulate F' , we
 942 must use exactly $f' + 2b' - 3$ edges. As done by our procedure of constructing G' , we have
 943 at most $2b'$ of these edges in $\Omega_i \cup P_{i'}$ - indeed, if we use an edge in Ω_i to replace two bridges
 944 by a block that is a triangle, then we later use (three) edges from Υ_i merge this block into
 945 the larger block. And for the other bridge edges, we put exactly two edges in Π_i . This leaves
 946 us with at least $f' - 3$ edges of $\Delta_i \cup \Upsilon_i$ embedded inside F' .



■ **Figure 17** An illustration of the fact that F'' cannot exist. The connected component of $B_{i'}$ that contains u is depicted by an oval with thin solid borders. The dashed straight segments are edges of the input graph G .

947 We pay all the edge of Γ_i that appear on the boundary of F' and are not bridges by
 948 charging the component of $B_{i'}$ that contains u and the edges of $\Delta_i \cup \Upsilon_i$ embedded inside
 949 F' . Note that as argued above, $B_{i'}$ cannot be charged more than once this way, and thus
 950 it brings 3 credits. Also, the edges of $\Delta_i \cup \Upsilon_i$ embedded inside F' are not charged in any
 951 other place, so they bring $2(f' - 3)$ credits. Then we have at least f' credits to pay for all
 952 the edges of Γ_i that appear on F' . We do this and then every edge of every Γ_i is paid one
 953 credit. In conclusion, the claim holds. ■

954 Using Inequality (21) in Inequality (20) we obtain:

$$\sum_{i=1}^c \left(\frac{2}{3} \alpha_i + 4n_i - 8 \right) \geq 2n - 4 - 2\theta - (10/3)c.$$

From this, the fact that $n_i = 1 + 3d_i + 2t_i$, and Inequality (18), we obtain:

$$\sum_{i=1}^c \left(\frac{2}{3} (3d_i - 2) + 4(1 + 3d_i + 2t_i) - 8 \right) \geq 2n - 4 - 2\theta - (10/3)c,$$

which simplifies to

$$\sum_{i=1}^c \left(14d_i + 8t_i - \frac{16}{3} \right) \geq 2n - 4 - 2\theta - (10/3)c.$$

This in turn simplifies to:

$$14d + 8t - (16/3)c \geq 2n - 4 - 2\theta - (10/3)c,$$

and using the early assumption that $c \geq 1$, this implies

$$7d + 4t \geq n - \theta - 1. \tag{24}$$

From Inequality (17) we obtain:

$$2n \geq 11d + 8t,$$

which is equivalent to

$$5(n - 7d - 4t) + 24d + 12t \geq 3n.$$

Using Inequality (24), this implies:

$$5\theta + 24d + 12t \geq 3n - 18.$$

which is equivalent to

$$\frac{(n - 1) + 2d + t}{3n - 6 - \theta} \geq \frac{5}{12}.$$

This completes the analysis of the algorithm LDT. We have:

► **Theorem 9.** *Algorithm LDT is an approximation algorithm with ratio of 5/12, and can be implemented to run in time $O(n^5)$.*

5 A Greedy Algorithm followed by LDT

In this section, we present Algorithm GDLDT (Greedy-Diamonds-Local-Diamonds-Triangles) that achieves a small improvement over Algorithm LDT from the previous section.

Algorithm GDLDT adds diamonds greedily as long as we can maintain a dt-structure¹² before we start Phase I of the LDT algorithm.

¹²As mentioned earlier, this is exactly the start of the GDT algorithm of [7].

3:34 Local Optimization Algorithms for Maximum Planar Subgraph

980 We end up with $k \geq 0$ non-trivial connected diamond-structures¹³ A_i each with d_i
 981 diamonds. A special case is $k = 0$; it will be discussed later. Recall that H is a triangulated
 982 plane graph that has all the edges of OPT and another set Δ of δ edges. We have $1 + 3d_i$
 983 vertices in A_i or in $B_i := H[V(A_i)]$. B_i would have at most $9d_i - 3$ edges. We define
 984 $d := \sum_{i=1}^k d_i$. Also let $BB := \cup_{i \in \{1, 2, \dots, k\}} E(B_i)$.

985 H has $3n - 6$ facial diamonds - one for every edge. Call a pair of facial diamonds
 986 *interlocking* if the base of one is an edge of another. Then one facial diamond participates in
 987 four pairs of interlocking facial diamonds.

988 No facial diamond of H can be added when **Greedy Diamonds** stops, and based on
 989 this we classify all the facial diamonds of H into one of the following three categories:

990 **Category I:** One edge of the facial diamond is in Θ (recall that Θ is a set of edges that are
 991 in H but not OPT , and that $\theta = |\Theta|$).

992 **Category II:** Not of Category I, and one edge of the facial diamond is in BB .

993 **Category III:** Not of Categories I and II, and the two tips of the facial diamond are in the
 994 same $V(B_i)$, for some $i \in \{1, 2, \dots, k\}$.

995 An edge e of Θ participates in at most 5 facial diamonds: one diamond D where the edge
 996 e is the base, and at most 4 facial diamonds where the base is one of the at most four edges
 997 other than e in the facial diamond that has e as a base. Thus there are at most 5Θ facial
 998 diamonds of Category I.

999 If $k = 0$ (the special case where no diamonds were found), then we only have facial
 1000 diamonds of Category I. Then we have

$$1001 \quad 5\theta \geq 3n - 6. \tag{25}$$

1002 From Inequality (24) (here $d = 0$), we obtain:

$$1003 \quad 4t \geq n - \theta - 1$$

1004 and therefore

$$1005 \quad \frac{n - 1 + 2d + t}{3n - 6 - \theta} \geq \frac{(5/4)n - (5/4) - (1/4)\theta}{3n - 6 - \theta} \geq \frac{11}{24} > \frac{91}{216},$$

1006 where the middle inequality above follows by simple algebra from Inequality (25).

1007 From now on, we assume that $k > 0$. Similarly, an edge of BB participates in at most 5
 1008 facial diamonds. Thus there are at most $5|BB|$ facial diamonds of Category II.

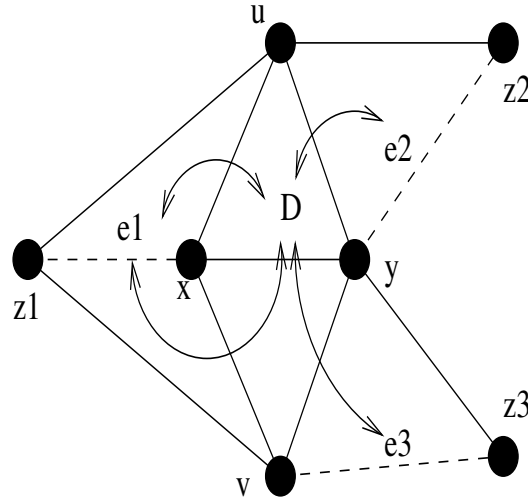
1009 Let us now consider the set of facial diamonds of Category III. If a facial diamond of
 1010 Category III belongs to interlocking pair of facial diamonds with another facial diamond of
 1011 Category III, then we put both these facial diamonds in a set Q . Let R be the set of facial
 1012 diamonds of Category III that were not put in Q .

1013 We construct a bipartite multigraph M with R as the vertices of one part, and $BB \cup \Theta$
 1014 as the vertices of the other part, and edge set defined as follows.

1015 Let D be a facial diamond of R with base vertices x and y and tips u and v . Note that
 1016 there is an i such that u and v are in $V(B_i)$ while x and y are not in $V(B_i)$. Consider the
 1017 four distinct facial diamonds of H with bases xu , yu , xv , and yv . As we assumed D is not in
 1018 Q , for each D' of these four facial diamonds, there must be an edge e of $\Theta \cup BB$ that makes
 1019 D' ineligible for being added by the Greedy algorithm (D' is of Category I or II since if D'
 1020 were to be of Category III, then D' and D would interlock). Put an edge in M between D

¹³A diamond structure is a graph whose blocks are all diamonds

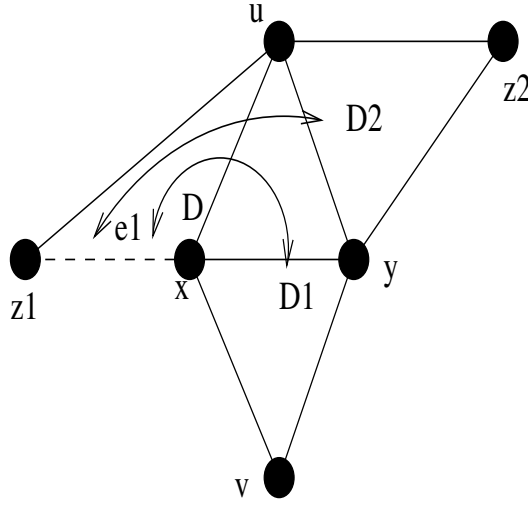
1021 and e and label this edge by D' . Do this for all the four diamonds interlocking with D . We
 1022 may end up putting two edges between D and some edge e of $\Theta \cup BB$, labeled by two distinct
 1023 diamonds that interlock with D and both contain e . See Figure 18 for an illustration. Note
 1024 that e is not the base of the facial diamond D' when an edge of M incident to e (seen as a
 1025 vertex of M) is labeled by D' .



■ **Figure 18** Straight segments, dashed or not, are edges of H . We have a diamond D that is in the set R , with base xy and tips u and v . There are four facial diamonds that interlock with D , and in this figure the facial diamonds with bases xu , xv , yu , and yv have tip set $\{z_1, y\}$, $\{z_1, y\}$, $\{z_2, x\}$, and $\{z_3, x\}$ respectively. Each of these four facial diamonds has one edge in $\Theta \cup BB$, which in this figure are the three dashed segments e_1 , e_2 , and e_3 . Then in M we put two edges with endpoints e_1 and D , one edge with endpoints e_2 and D , and one edge with endpoints e_3 and D . These edges of M are represented by arcs with arrows on both ends.

1026 Thus in M , every vertex that is a facial diamond of R has degree exactly four. An edge e
 1027 of $\Theta \cup BB$, seen as a vertex of M , cannot gain more than one edge of M labeled by diamond
 1028 D' (here D' must contain e), since e is not the base of D' and if two facial diamonds of
 1029 R , say, D_1 and D_2 will get an edge to e in M labeled D' , then D_1 and D_2 interlock (see
 1030 Figure 19) and thus they are not in R . Thus a vertex of M that is an edge e of $\Theta \cup BB$ has
 1031 degree at most four in M . By counting the degrees of the vertices of M , we conclude that:

1032 $|R| \leq |BB| + \theta.$ (26)



■ **Figure 19** Here D is the facial diamond with bases x and y and tips u and v . Assume that D is a member of R . As we construct the graph M , we put an edge between D and e , and we label this edge D' . Here e is the edge between w and x , and D' is the facial diamond of H with bases x and u and tips y and w . The only other facial diamond that could have an edge of M labeled D' incident to e is D_2 , but then D_2 and D_1 interlock and none of them would be a member of R .

1033 Let $AA := E(H[\cup_{i \in \{1,2,\dots,k\}} V(A_i)])$, where we recall that k is the number of non-
 1034 trivial components A_i . Also recall that $BB = \cup_{i \in \{1,2,\dots,k\}} E(B_i)$ and $B_i = H[V(A_i)]$; thus
 1035 $BB \subseteq AA$. We will construct a bipartite graph M' with the left part being the edges of
 1036 $AA \setminus BB$ and the right part being the diamonds of Q .

1037 Consider now a facial diamond D_1 from Q . Let D_1 have base vertices x and y and tips
 1038 u and v . Note that there is an i such that u and v are in $V(B_i)$ while x and y are not in
 1039 $V(B_i)$. Since $D_1 \in Q$, there is a diamond D_2 of Category III that interlocks with D_1 ; wlog
 1040 we assume that D_2 has base uy and tips x and z . See Figure 19 for an illustration, ignoring
 1041 the vertex w and the diamond D' . Then there exists $j \neq i$ with vertices x and z in $V(B_j)$.
 1042 Note then that ux and xv are edges of $AA \setminus BB$. We put in M' edges from D_1 to the edges
 1043 ux and xv . Note that neither ux nor xv is the base edges of D_1 . Thus every vertex in the
 1044 right part of the bipartite graph M' has degree exactly 2. An edge of $AA \setminus BB$ appears as a
 1045 non-base edge in four diamonds of H and thus, seen as a vertex in the left part of M' , can
 1046 have degree at most 4. We conclude:

1047
$$|Q| \leq 2|AA \setminus BB| = 2|AA| - 2|BB|.$$

1048 As every facial diamond of H belongs to one of the three categories, using the equation
 1049 above and Equation (26), we conclude:

1050
$$3n - 6 \leq 5\theta + 5|BB| + |R| + |Q| \leq 6\theta + 6|BB| + 2(|AA| - |BB|) = 6\theta + 4|BB| + 2|AA|. \quad (27)$$

1051 Now, since B_i is a simple planar graph with $1 + 3d_i$ vertices, we have $|E(B_i)| \leq 9d_i - 3$.
 1052 Note also that $|BB| = \sum_{i=1}^k |E(B_i)| \leq 9d - 3k$. The set AA is the edge set of a planar graph
 1053 with $\sum_{i=1}^k (1 + 3d_i) = k + 3d$ vertices and therefore $|AA| \leq 3(k + 3d) - 6 = 9d + 3k - 6$.
 1054 Using these inequalities and Inequality (27) we obtain:

1055
$$3n - 6 \leq 6\theta + 4(9d - 3k) + 2(9d + 3k - 6) = 6\theta + 54d - 12 - 6k.$$

1056 This implies

$$1057 \quad d \geq \frac{1}{18}n - \frac{1}{9}\theta.$$

1058 Adding this to Inequality (24), we obtain:

$$1059 \quad 8d + 4t \geq \frac{19}{18}n - \frac{10}{9}\theta - 1,$$

1060 which leads to

$$1061 \quad 2d + t \geq \frac{19}{72}n - \frac{5}{18}\theta - \frac{1}{4}.$$

1062 Using $\theta \geq 0$, one can verify that this implies:

$$1063 \quad \frac{n - 1 + 2d + t}{3n - 6 - \theta} \geq \frac{91}{216},$$

1064 which is still far from $3/7$ but is a little bit better than $5/12$. In conclusion we have the first
1065 statement of:

1066 ► **Theorem 10.** *Algorithm GDLDT (greedily adding diamonds followed by our LDT algorithm)*
1067 *is an approximation algorithm with ratio of at least $91/216$, and at most $3/7$, and can be*
1068 *implemented to run in time $O(n^5)$.*

1069 Regarding the running time, there are $O(n^4)$ diamonds and it is straightforward to use
1070 connected components to check whether a diamond can be greedily added in time $O(n^4)$.
1071 There are at most $O(n)$ such additions. Algorithm LDT can be implemented to run in time
1072 $O(n^5)$. The second statement of the theorem is proved ahead.

1073 5.1 Upper bound on the approximation ratio

1074 We do not have a matching upper bound for the algorithm discussed in this section. However
1075 the ratio will not exceed $3/7 < 4/9$, as shown in the following example.

1076 Consider a dt-structure D with d diamonds and no triangles; moreover the d diamonds
1077 are connected so that the edges between the bases of each diamond form a tree T . So T has
1078 $d + 1$ vertices; there are another $2d$ tips. Arrange the $2d$ tips as our graph H from the $5/12$
1079 example and, just like there, add a new vertex in every second face of H , making it adjacent
1080 to the three vertices of H bordering that face. Construct a triangulated planar graph J on
1081 the $d + 1$ vertices of $V(T)$. Then add a new vertex in every face of J , connecting it to the
1082 three vertices of J bordering the face. The dt-structure D together with H and J and the
1083 new vertices form the input graph G . There are $2d - o(d)$ new vertices in the faces of H and
1084 $2d - 2$ new vertices in the faces of J ; so G has $7d - o(d)$ vertices. Graph H combined with
1085 its new vertices is planar and has $4d - o(d)$ vertices and $12d - o(d)$ edges, and J combined
1086 with its new vertices is planar and has $3d - 1$ vertices and $9d - 9$ edges, and thus a planar
1087 subgraph of G with $21d - o(d)$ edges exists.

1088 Just like in the $5/12$ series of examples, one can check that D cannot be improved by the
1089 local optimization step. Then our output will have at most $7d + 2d$ edges (two extra edges
1090 for each diamond). By choosing d as large as we wish, we get a ratio as close to $9/21 = 3/7$
1091 as we want.

1092 A variation of this example gives an upper bound of $11/27 < 5/12$ for the algorithm of [7]
1093 which greedily adds diamonds followed by greedily adding triangles: put a new vertex in all
1094 the faces of H , not just half of them. We end up with $6d - o(d)$ new vertices, for a total of
1095 $9d - o(d)$ vertices and a planar subgraph with $27d - o(d)$ edges. The output will have at
1096 most $9d + 2d$ edges as no triangle can be added to the d diamonds of D .

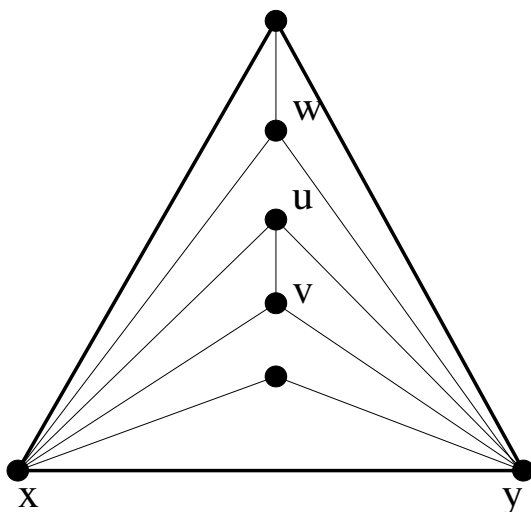
1097 **6** Conclusions and Discussion

1098 We improved the approximation ratio for Maximum Planar Subgraph from $4/9$ to $4/9 + \epsilon$,
 1099 for a very small $\epsilon > 0$, by analyzing the application of a natural local optimization step
 1100 after applying the previously known, Matroid-Parity based $(4/9)$ -approximation algorithm.
 1101 Our analysis, while involved, is not tight and there may be room for a more significant
 1102 improvement here.

1103 In particular, we do not believe that Equation (13) is tight. We conjecture that the tight
 1104 (excluding a small additive term) bound that generalizes Theorem 5 is:

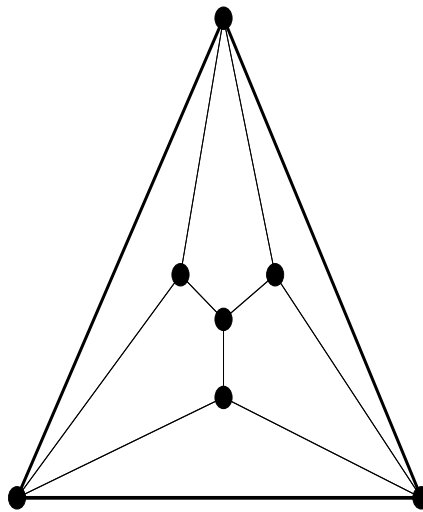
$$1105 \quad \Phi(\mathcal{P}, \mathcal{Q}) \geq \frac{3}{7}n - \frac{1}{7}c - \frac{10}{21}t \quad (28)$$

1106 Here we are looking at double-partitions $(\mathcal{P}, \mathcal{Q})$ that cover all the facial triangles of a plane
 1107 graph H with n vertices and t is the number of edges missing from H to be a triangulation.
 1108 As before, c is the number of cubic vertices in H , but without H being triangulated, we
 1109 provide a new definition of cubic, as follows. Say vertex v is adjacent to u, x, y forming a
 1110 K_4 with v embedded strictly inside the triangle uxy . We call v cubic if none of the three
 1111 triangles vux, vxy, vyu have a vertex z strictly inside that forms a K_4 with its neighbors.
 1112 See Figure 20 for an example. This bound would be tight, as described next.



■ **Figure 20** Here v is a cubic while w is not.

1113 Consider a triangulation W on r vertices containing no K_4 . Add four vertices in each
 1114 face as in Figure 21. We have $n = r + 4(2r - 4) = 9r - 16$ and $t = 3(2r - 4) = 6r - 12$. There
 1115 are no K_4 's and therefore no cubic vertices in this graph. Choose \mathcal{P} to have one non-trivial
 1116 vertex class: W , and \mathcal{Q} has no non-trivial edge color, so that $\Phi(\mathcal{P}, \mathcal{Q}) = r - 1$. One can
 1117 verify that all the triangles are covered by double-partition $(\mathcal{P}, \mathcal{Q})$. Then, as r increases,
 1118 Equation (28) becomes tight.



■ **Figure 21** Faces used to show tightness of Equation (28).

1119 Equation (28) would allow us to increase the ϵ to maybe $1/270$ with the current techniques.

1120 We also presented a local optimization algorithm, LDT, that does not use Matroid Parity
 1121 and has a tight approximation bound of $5/12$. Applying a greedy algorithm before starting this
 1122 second local optimization gives a small improvement, to at least $91/216 = (5/12) + (1/216)$.
 1123 Consider the following variant of our LDT algorithm: the algorithm keeps a dt-structure,
 1124 and a local optimization step would either add a triangle, replace a triangle by a diamond,
 1125 or replace a diamond by a diamond and a triangle. This variant has approximation ratio of
 1126 at least $5/12$, as all the local steps LDT makes are done by the variant. Moreover, the series
 1127 of examples showing that LDT has approximation ratio at most $5/12$ holds for this variant.
 1128 And if we augment the variant to add diamonds before adding triangles, then we get a ratio
 1129 between $91/216$ and $3/7$ as we did for GDLDT.

1130 As in the previous work [5], we use the approach of using a few basic graphs for blocks in
 1131 our output. This guarantees planarity and is at the basis of the analysis of all approximation
 1132 algorithms for MPS with ratio bigger than $1/3$. As long as one uses this approach, this paper
 1133 suggests that the application of local optimization, even if it comes before or after other
 1134 algorithms, is beneficial, and more powerful than Greedy algorithms (albeit slower).

1135 If we are to use blocks of fixed size, it is not hard to see and known since [3] that one
 1136 cannot achieve an approximation better than $1/2$. But maybe the “spruces” of [6] can give
 1137 us $1/2$ or better if used as the blocks of output.

1138 One approach that does not use Matroid Parity, and we were not able to analyze beyond
 1139 the $91/216$ bound presented earlier outputs a 4-structure by:

- 1140 1. Use the approximation algorithm of [22] to get a $((2/3) - \epsilon)$ -approximation for the
 1141 maximum K_4 -structure. Contract the selected K_4 's.
- 1142 2. Use again the approximation algorithm of [22] to get a $((2/3) - \epsilon)$ -approximation for the
 1143 maximum diamond-structure.
- 1144 3. Use our LDT algorithm. Add to it three other local “new” optimizations steps:
 - 1145 – If one can replace two triangles by a diamond and still have a 4-structure, do so;
 - 1146 – If one can replace three triangles by a K_4 and still have a 4-structure, do so;
 - 1147 – If one can replace one triangle and one diamond by a K_4 and still have a 4-structure,
 1148 do so;

3:40 Local Optimization Algorithms for Maximum Planar Subgraph

1149 4. Contract the blocks and use once again the approximation algorithm of [22] to get a
1150 $(2/3) - \epsilon$ approximation for the maximum C_4 -structure.

1151 5. Expand everything contracted and connect the blocks with bridges to output a connected
1152 graph.

1153 Maybe this or a variant of this can also beat the $4/9$ ratio. The three new local optimization
1154 steps mentioned above do not increase the cyclomatic number but may be useful as they
1155 increase the number of connected components in our 4-structure.

1156 An alternative would be to devise an approximation algorithm for Weighted Matroid
1157 3-Parity, when the weights are 3 (from K_4 's), 2 (from diamonds), and 1 (from triangles and
1158 C_4 's). With such small integer weights, again local optimization seems the way to go.

1159 — References —

- 1160 1 Markus Blaeser, Gorav Jindal, and Anurag Pandey. A deterministic PTAS for the commutative
1161 rank of matrix spaces. *Theory of Computing*, 14:1–21, 01 2018. doi:10.4086/toc.2018.
1162 v014a003.
- 1163 2 Jiazhen Cai, Xiaofeng Han, and Robert E Tarjan. An $O(m \log n)$ -time algorithm for the
1164 maximal planar subgraph problem. *SIAM Journal on Computing*, 22(6):1142–1162, 1993.
- 1165 3 Gruia Călinescu and Cristina G. Fernandes. On the k -structure ratio in planar and outerplanar
1166 graphs. *Discrete Mathematics & Theoretical Computer Science*, 10(3):135–148, 2008. URL:
1167 <http://www.dmtcs.org/dmtcs-ojs/index.php/dmtcs/article/view/961/2387>.
- 1168 4 Gruia Călinescu and Cristina G. Fernandes. Maximum planar subgraph. In Teofilo F. Gonzalez,
1169 editor, *Handbook of Approximation Algorithms and Metaheuristics, Second Edition, Volume 2:
1170 Contemporary and Emerging Applications*. Chapman and Hall/CRC, 2018.
- 1171 5 Gruia Călinescu, Cristina G. Fernandes, Ulrich Finkler, and Howard J. Karloff. Better
1172 approximation algorithm for finding planar subgraphs. *Journal of Algorithms*, 27(2):269–302,
1173 1998.
- 1174 6 Gruia Călinescu, Cristina G. Fernandes, Hemanshu Kaul, and Alexander Zelikovsky. Maximum
1175 series-parallel subgraph. *Algorithmica*, 63(1-2):137–157, 2012.
- 1176 7 Parinya Chalermsook and Andreas Schmid. Finding triangles for maximum planar sub-
1177 graphs. In Sheung-Hung Poon, Md. Saidur Rahman, and Hsu-Chun Yen, editors, *WALCOM:
1178 Algorithms and Computation*, pages 373–384, 2017.
- 1179 8 Parinya Chalermsook, Andreas Schmid, and Sumedha Uniyal. A tight extremal bound on
1180 the Lovász cactus number in planar graphs. In *36th International Symposium on Theoretical
1181 Aspects of Computer Science*, 2019.
- 1182 9 Ho Yee Cheung, Lap Chi Lau, and Kai Man Leung. Algebraic algorithms for linear matroid
1183 parity problems. *ACM Transactions on Algorithms (TALG)*, 10(3):1–26, 2014.
- 1184 10 T Chiba, I Nishioaka, and I Shirakawa. An algorithm of maximal planarization of graphs. In
1185 *Proc. IEEE Symp. on Circuits and Systems*, pages 649–652, 1979.
- 1186 11 Markus Chimani, Ivo Hedtke, and Tilo Wiedera. Limits of greedy approximation algorithms
1187 for the maximum planar subgraph problem. In *Combinatorial Algorithms: 27th International
1188 Workshop, IWOCA 2016, Helsinki, Finland, August 17-19, 2016, Proceedings 27*, pages 334–346.
1189 Springer, 2016.
- 1190 12 Markus Chimani, Ivo Hedtke, and Tilo Wiedera. Exact algorithms for the maximum planar
1191 subgraph problem: New models and experiments. *Journal of Experimental Algorithmics (JEA)*,
1192 24:1–21, 2019.
- 1193 13 Markus Chimani, Karsten Klein, and Tilo Wiedera. A note on the practicality of maximal
1194 planar subgraph algorithms. In Yifan Hu and Martin Nöllenburg, editors, *Graph Drawing and
1195 Network Visualization*, pages 357–364, Cham, 2016. Springer International Publishing.
- 1196 14 Markus Chimani and Tilo Wiedera. Cycles to the rescue! novel constraints to compute
1197 maximum planar subgraphs fast. In Yossi Azar, Hannah Bast, and Grzegorz Herman, editors,
1198 *26th Annual European Symposium on Algorithms, ESA 2018, August 20-22, 2018, Helsinki,
1199 Finland*, volume 112 of *LIPICs*, pages 19:1–19:14. Schloss Dagstuhl - Leibniz-Zentrum für
1200 Informatik, 2018. doi:10.4230/LIPICs.ESA.2018.19.
- 1201 15 Robert Cimikowski. An analysis of heuristics for graph planarization. *Journal of Information
1202 and Optimization Sciences*, 18(1):49–73, 1997.
- 1203 16 M.E. Dyer, L.R. Foulds, and A.M. Frieze. Analysis of heuristics for finding a maximum weight
1204 planar subgraph. *European Journal of Operations Research*, 20:102–114, 1985.
- 1205 17 Leslie R Foulds. *Graph theory applications*. Springer Science & Business Media, 2012.
- 1206 18 Harold N. Gabow and Matthias F. Stallmann. An augmenting path algorithm for linear
1207 matroid parity. *Combinatorica*, 6:123–150, 1986.
- 1208 19 H.N. Gabow and M. Stallmann. Efficient algorithms for graphic matroid intersection and
1209 parity. In *12th Colloq. on Automata, Language and Programming*, pages 210–220, 1985.

- 1210 20 M. R. Garey and D. S. Johnson. *Computers and Intractability*. W.H. Freeman and Co., NY,
1211 1979.
- 1212 21 M. Junger and P. Mutzel. Maximum planar subgraphs and nice embeddings: Practical layout
1213 tools. *Algorithmica*, 16:33–59, 1996.
- 1214 22 Jon Lee, Maxim Sviridenko, and Jan Vondrák. Matroid matching: The power of local
1215 search. *SIAM Journal on Computing*, 42(1):357–379, 2013. arXiv:[https://doi.org/10.](https://doi.org/10.1137/11083232X)
1216 [1137/11083232X](https://doi.org/10.1137/11083232X), doi:10.1137/11083232X.
- 1217 23 Annegret Liebers. Planarizing graphs—a survey and annotated bibliography. In *Graph*
1218 *Algorithms And Applications 2*, pages 257–330. World Scientific, 2004.
- 1219 24 P.C. Liu and R.C. Geldmacher. On the deletion of nonplanar edges of a graph. In *10th*
1220 *Southeastern Conference on Combinatorics, Graph Theory, and Computing*, pages 727–738,
1221 1977.
- 1222 25 L. Lovász and M.D. Plummer. *Matching theory*. North-Holland, Amsterdam–New York, 1986.
- 1223 26 James B Orlin. A fast, simpler algorithm for the matroid parity problem. In *International*
1224 *Conference on Integer Programming and Combinatorial Optimization*, pages 240–258. Springer,
1225 2008.
- 1226 27 Timo Poranen. A simulated annealing algorithm for the maximum planar subgraph problem.
1227 *International Journal of Computer Mathematics*, 81(5):555–568, 2004.
- 1228 28 Timo Poranen. Two new approximation algorithms for the maximum planar subgraph problem.
1229 *Acta Cybernetica*, 18(3):503–527, 2008. URL: [https://cyber.bibl.u-szeged.hu/index.php/](https://cyber.bibl.u-szeged.hu/index.php/actcybern/article/view/3735)
1230 [actcybern/article/view/3735](https://cyber.bibl.u-szeged.hu/index.php/actcybern/article/view/3735).
- 1231 29 A. Schrijver. *Combinatorial Optimization*. Springer, 2003.
- 1232 30 Z. Szigeti. On the graphic matroid parity problem. *J. Combin. Theory Ser. B*, 88:247–260,
1233 2003.
- 1234 31 Roberto Tamassia. Graph drawing. In *Handbook of computational geometry*, pages 937–971.
1235 Elsevier, 2000.
- 1236 32 Douglas B. West. *Introduction to Graph Theory*. Prentice Hall, 2 edition, September 2000.